

# Uncertainty Quantification on Graph Learning: A Survey

Chao Chen<sup>†</sup>, Chenghua Guo<sup>†</sup>, Rui Xu<sup>†</sup>, Xiangwen Liao, Xi Zhang, *Member, IEEE*,  
Sihong Xie\*, Hui Xiong, *Fellow, IEEE*, Philip S. Yu *Fellow, IEEE*

**Abstract**—Graphical models have demonstrated their exceptional capabilities across numerous applications, such as social networks, citation networks, and online recommendation systems. Despite these successes, their performance, confidence, and trustworthiness are often limited by the inherent randomness of data in nature and the challenges of accurately capturing and modeling real-world complexities. This has increased interest in developing uncertainty quantification (UQ) techniques tailored to graphical models. In this survey, we comprehensively examine these existing works on UQ in graphical models, focusing on key aspects such as foundational knowledge, sources, representation, handling, and measurement of uncertainty. This survey distinguishes itself from most existing UQ surveys by specifically concentrating on UQ in graphical models, particularly probabilistic graphical models (PGMs) and graph neural networks (GNNs). We elaborately categorize recent work into two primary areas: uncertainty representation and uncertainty handling. By offering a comprehensive overview of the current landscape, including both established methodologies and emerging trends, we aim to bridge gaps in understanding and highlight key challenges and opportunities in the field. Through in-depth discussion of existing works and promising directions for future research, we believe this survey serves as a valuable resource for researchers, inspiring them to cope with uncertainty issues in both academic research and real-world applications.

**Index Terms**—Article submission, IEEE, IEEEtran, journal, L<sup>A</sup>T<sub>E</sub>X, paper, template, typesetting.

## I. INTRODUCTION

Graphical models have emerged as fundamental tools in machine learning due to their capability to capture and manage complex relational dynamics among variables. These models have found extensive applications in various domains and tasks, such as spam detection in online review systems [1], [2], relationship extraction in social networks [3]–[6], interest exploration in recommendation systems [7]–[10], and drug discovery in protein-protein interaction networks [11]–[13]. Unlike traditional models, where variables are assumed to be independently and identically distributed (i.i.d.), graphical models reveal intricate relationships and conditional dependencies. Considering both individual variables and their interconnections, graphical models improve predictive performance in complex data environments and tasks.

However, uncertainties are ubiquitous and can arise from various sources, including inherent data randomness, model

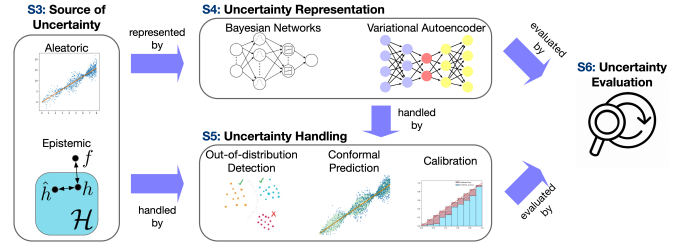


Fig. 1. Overview of the uncertainty quantification: the survey introduces the source of uncertainty in Sec. III. Then, the state-of-the-art methods proposed for uncertainty representation and handling are demonstrated in Sec. IV and Sec. V, respectively. To assess the results of UQ, the evaluation protocols on UQ will be presented in Sec. VI.

training errors, and unexpected test data distributions [14]. These uncertainties hinder the application of graphical models in critical fields where precise risk assessment and decision-making under uncertainty are essential. Quantifying uncertainty (UQ) provides confidence measures and explanations alongside predictions, enhancing the reliability and safety of models in practice. Thus, many works have focused on developing UQ methods specifically for graphical models, allowing their applications in domains such as healthcare [15] and autonomous driving [16].

This survey explores various types of uncertainties in two primary types of graphical models: graph neural networks (GNNs) and probabilistic graphical models (PGMs). GNNs extend the successes of deep learning to graph-structured data but face challenges such as noisy links, missing nodes, or mislabeled data. Recent developments have incorporated uncertainty quantification into the architectures and training algorithms of GNNs, improving their robustness and interoperability. PGMs, including Bayesian Networks and Markov Random Fields, utilize more rigorous probabilistic formulations to effectively represent uncertainty and are particularly effective in scenarios requiring joint probability modeling and causal relationship analysis.

Existing surveys on UQ can be categorized based on their focus, such as their specific application domain (e.g., UQ for graph learning), and the breadth of their coverage, ranging from comprehensive overviews of UQ methods to in-depth explorations of particular UQ techniques. The survey most closely related to the present survey is [14], which also focuses on graph learning and UQ. Similarly to our survey, [14] investigates the sources of uncertainty, evaluation methods, and various techniques for handling uncertainty in graph

<sup>†</sup> Three authors are listed in alphabetical order with equal contributions to this work. Specifically, Chao primarily focused on Sec. II, Sec. V-A and Sec. V-B; Chenghua primarily worked on Sec. IV; and Rui primarily handled Sec. III, Sec. V-B, Sec. V-C, and Sec. VI.

\*Corresponding author: sihongxie@hkust-gz.edu.cn

TABLE I  
NOTATION DEFINITIONS

$G = (\mathcal{V}, \mathcal{E})$	A graph with node set $\mathcal{V}$ and edge set $\mathcal{E}$ .
$V_i \in \mathcal{V}$	A node with features in the graph.
$X_i$	Node feature vector of node $V_i$ .
$Y_i \in \mathcal{Y}$	Ground truth of node $V_i$ .
$\hat{Y}_i \in \mathcal{Y}$	Approximation of node $V_i$ .
$K$	The number of classes in a classification task.
$\mathcal{N}(V_i)$	Direct neighbors of node $V_i$ .
$f(\theta) \in \mathcal{F}$	A model $f$ with parameters $\theta$ from a function space $\mathcal{F}$ .
$P_*, P_0$	Real and observed data distribution.
$x_i, y_i$	A specific value of $X_i$ and $Y_i$ , respectively.

learning. However, a key distinction between [14] and our survey is that the former does not include a discussion on the representation methods for uncertainty. In broader application domains, some surveys provide comprehensive coverage of UQ methods. For example, [17]–[20] explore uncertainty in deep learning, while [21] examines uncertainty in scientific machine learning. These surveys provide valuable insights into UQ across different application domains. However, they do not specifically delve deep into the uncertainty in graph learning. Furthermore, several surveys offer an in-depth analysis of specific aspects of UQ, such as sources of uncertainty [22], [23], optimization under uncertainty [24], noise in machine learning [25], but do not focus on uncertainty in graph learning. Despite the valuable contributions of the existing work mentioned above, they collectively lack a comprehensive overview of uncertainty quantification on graph learning.

This survey aims to review various strategies and methodologies to model, measure, and mitigate uncertainty in GNNs and PGMs. By examining recent research, including state-of-the-art works, the survey provides a comprehensive understanding of how current research addresses uncertainty and forecasts future enhancements to increase their efficacy. Specifically, this survey organizes the literature on uncertainty in graphs into four main parts, as demonstrated in Fig. 1. Specifically, we first provide the preliminary knowledge concerning PGMs and GNNs in Sec. II, and introduce the sources of uncertainty in Sec. III. We then discuss the methods used for uncertainty representation in Sec. IV and uncertainty handling in Sec. V. Table. II categorizes these UQ techniques by their properties. For instance, we are interested in whether they involve model training or post-hoc, whether they are based on uncertainty or deterministic parameters, and whether they have impacts on accuracy performance. Additionally, we will demonstrate widely used metrics for uncertainty evaluation in Sec. VI. Finally, the conclusion of the survey will be made in Sec. VIII.

## II. PRELIMINARIES

### A. Basic Notations for Graphs

We summarize the formal notations for key definitions and variables in Table I. Consider a graph  $G = (\mathcal{V}, \mathcal{E})$  consisting of a set of  $n$  nodes  $\mathcal{V} = \{V_1, \dots, V_n\}$ , each representing a random variable, and each variable  $V_i \in \mathcal{V}$  is associated with a feature vector  $X_i$ . The “feature” could be a prior distribution indicating the likelihood of belonging to class  $k$  (typically in

MRF cases), or a vector with practical meanings, such as bag-of-words (typically in GNN cases). Each edge in the set of edges  $\mathcal{E}$  is a relationship between two variables. The set  $\mathcal{N}(V_i)$  collects direct neighbors of  $V_i$ , e.g.,  $\mathcal{N}(V_i) = \{V_j : (V_i, V_j) \in \mathcal{E}\}$ . In the node classification task, for each unlabeled variable  $V_i$ , the model aims to estimate its probability distribution  $\hat{Y}_i$  and predict its label  $k_i$  out of  $K$  possible classes.

### B. Probabilistic Graphical Model

A probabilistic graphical model (PGM) [26], [27] is widely used to represent the joint probability distribution of random variables, whose relations can be depicted in a graph. There are two distinct categories of PGMs, depending on whether the graph’s edges are directed or undirected. Specifically, a Bayesian Network is employed for modeling a directed graph, where edges represent causality. Conversely, a Markov Random Field (MRF) is utilized to model an undirected graph, where edges signify the correlation between nodes. An MRF factorizes the joint distribution  $P(\mathcal{V})$  as

$$P(\mathcal{V}) = \frac{1}{Z} \prod_{V_i \in \mathcal{V}} \phi(X_i = x_i) \prod_{V_j \in \mathcal{N}(V_i)} \psi(X_i = x_i, X_j = x_j), \quad (1)$$

where  $Z$  normalizes the product to a probability distribution.  $\phi(X_i = x_i)$  denotes the prior probability of  $X_i$  taking value  $x_i$ , independent of other variables. The compatibility  $\psi(X_i = x_i, X_j = x_j)$  represents the preference of the pair  $(x_i, x_j)$  occurring jointly, capturing the dependencies between the two variables. The marginal distribution  $b(X_i)$  for  $V_i \in \mathcal{V}$  is

$$b(X_i = x_i) = \sum_{\mathcal{V} \setminus X_i} P(\mathcal{V} \setminus X_i, X_i = x_i). \quad (2)$$

### C. Graph Neural Networks

Unlike traditional neural networks that operate on grid-like data (such as tabular vectors, images, or sequences), graph neural network (GNN) could learn from complex relationships and dependencies in graphs. Formally, for the  $l$ -th layer of an  $L$ -layers GNN, the node representation  $\mathbf{h}_i^{(l)}$  for node  $V_i$  is calculated by

$$\mathbf{a}_i^{(l)} = \text{AGG} \left( \left\{ \mathbf{h}_j^{(l-1)} \mid V_j \in \mathcal{N}(V_i) \right\} \right), \quad (3)$$

$$\mathbf{h}_i^{(l)} = \text{UPDATE} \left( \mathbf{a}_i^{(l)}, \mathbf{h}_i^{(l-1)} \right). \quad (4)$$

The AGG function aggregates the messages sent from all neighbors  $V_j \in \mathcal{N}(V_i)$  to  $V_i$ . It could operate the element-wise average, maximum over the message set, or employ a parametric layer for aggregation [28]. The UPDATE function combines representations of node  $X_i$  and its neighbors.  $\mathbf{h}_i^{(0)}$  is the input node feature for node  $X_i$ .  $\mathbf{h}_i^{(L)}$  can be softmaxed to a probability distribution for node-classification tasks, or be mapped to graph representation by a READOUT function for graph-level tasks. The parameters of GNN,  $\theta = \{\theta^{(l)}, l = 1, \dots, L\}$ , are trained in an end-to-end fashion.

### III. SOURCES OF UNCERTAINTY

The total uncertainty in machine learning can be decomposed into **aleatoric uncertainty** and **epistemic uncertainty** based on their sources [29]. Aleatoric uncertainty, which is irreducible with increasing amount of data, represents the randomness inherent to the data generation process [30]. However, epistemic uncertainty can be reduced by obtaining more knowledge or data to estimate the ground truth of predictions better [23], [31]. The techniques for the disentanglement of aleatoric and epistemic uncertainty are introduced by [32], and [33] formulate mathematical expressions of these two kinds of uncertainties in the context of GNNs.

The identification of aleatoric and epistemic uncertainty must be built upon the context of the selected model and available data [34]. For example, flipping a coin is usually regarded as a purely random event, involving aleatoric uncertainty. However, if we know the entire physics process of flipping a coin, including the flipping force, the coin's mass, volume, initial position, etc, we can simulate the process and predict whether it would be head or tail. Based on the simulation, the randomness can be regarded as epistemic uncertainty and can be reduced or even eliminated.

Focusing on supervised machine learning, we further explore the possible sources of uncertainty and how they impact prediction reliability. Let  $X \in \mathcal{X}$  and  $Y \in \mathcal{Y}$  denote input feature variable and the output label variable with realizations  $x$  and  $y$  respectively. The underlying data distribution is  $P_{XY}$  and the data generation mechanism is  $f$  such that  $y = f(x)$ .

#### A. Aleatoric Uncertainty

Aleatoric uncertainty is only about data noises, so we do not need to consider the influence of model selection and training issues and can investigate this problem under the view of statistics. According to [22], when  $f$  is conditioned on  $X = x$ , aleatoric uncertainty is the conditional probability distribution of  $Y$ , and its variance,  $Var_{Y|X}(Y|x)$ , can be used to quantify:

$$Y|x \sim P_{Y|X}(\cdot|X = x). \quad (5)$$

Four sources of aleatoric uncertainty are briefly introduced below. We refer the readers to [22] for a more comprehensive and detailed taxonomy.

**Omitted Features:** Omitted features, which are investigated in the context of causal models [35], confounder analysis [36], and model sensitivity analysis [37], are significant sources of aleatoric uncertainty. The omission can be caused by unobservability of data or overlooking during data collection. Let  $Z \in \mathcal{Z}$  denote an unobserved variable that influences the value of  $Y$ , we can see the expectation of  $Y|x$  is a weighted integration of  $\mathbb{E}_{Y|X,Z}$  on  $Z$ :

$$\begin{aligned} \mathbb{E}_{Y|X}[Y|x] &= \int_{y \in \mathcal{Y}} \int_{z \in \mathcal{Z}} y P_{Y|X,Z}(y|x, z) P_{Z|X}(z|x) dz dy \\ &= \int_{z \in \mathcal{Z}} \mathbb{E}_{Y|X,Z}[Y|x, z] P_{Z|X}(z|x) dz. \end{aligned} \quad (6)$$

In [22], the authors also claim that  $Var_{Y|X,Z}(Y|x, z) \leq Var_{Y|X}(Y|x)$  with at least one  $z \in \mathcal{Z}$ , indicating that

including the non-negligible variables will reduce aleatoric uncertainty.

**Feature Errors:** We will likely lose information with improper measurements, like low-resolution cameras, low-quality audio recorders, and uncalibrated gauges. These errors can cause biases and increased variance in feature collection. The authors of [25] reviewed 79 works on identifying and handling data noise. Here we let  $Z$  represent feature variables by faultless measurements and  $X$  denote those by inaccurate measurements, assuming that  $Y$  is independent of  $X|Z$ . According to [22], the change of aleatoric uncertainty caused by noisy feature values is illustrated as

$$Var_{Y|X}(Y|x) = \mathbb{E}_{Z|X}[Var_{Y|Z}(Y|Z)|x] + Var_{Z|X}(\mathbb{E}_{Y|Z}[Y|Z]|x). \quad (7)$$

The first term of the right-hand side is the expectation of  $Var_{Y|Z}(Y|Z)$  conditioned on  $X = x$ , and the second term is an increment in aleatoric uncertainty.

**Label Errors:** Label errors can be introduced by human labeling with subjectivity. Label errors in training sets will deviate models from correct gradient descent directions, and those in test sets will improperly evaluate models' performance. In [38], the authors state that at least 3.3% error rate across the most commonly-used computer vision, natural language, and audio datasets. If  $Z$  is the correct label variable and  $Y$  is the error-prone one, Eq. (5) can be rewritten as

$$Y|x \sim P_{Y|X}(\cdot|x) = \int_{z \in \mathcal{Z}} P_{Y|X,Z}(\cdot|x, z) P_{Z|X}(z|x) dz. \quad (8)$$

**Missing Data:** Missing data indicates some entries in the dataset are incomplete [39]. If  $(x_i, y_i)$  is the  $i$ -th sample of the dataset,  $M_i$  is its corresponding missing indicator.  $M_i = 0$  means the sample is complete, and  $M_i = 1$  otherwise. A bias factor is explained in [22] as  $\frac{P(M=0|y,x)}{P(M=0|x)}$  to express the influence from incompleteness by

$$P_{Y|X,M}(y|x, M=0) = \frac{\Pr(M=0|y,x)}{\Pr(M=0|x)} P_{Y|X}(y|x). \quad (9)$$

#### B. Epistemic Uncertainty

Epistemic uncertainty is introduced by model selection and training, rooted in the lack of data and knowledge. In [23], epistemic uncertainty is decomposed into model and approximation uncertainty. Let  $f \in \mathcal{F}$  be the ground truth mapping relationship from  $X$  to  $Y$ ,  $h \in \mathcal{H} \subset \mathcal{F}$  be the best possible predictor we can get, and  $\hat{h} \in \mathcal{H}$  be the induced predictor in practice.

**Model Uncertainty** measures the difference between  $f$  and  $h$ . This is because we can only explore a limited function space  $\mathcal{H}$ , which may not include the true  $f$ . Therefore, there can be a distance between the optimally trained predictor and the real mapping function. Taking  $l$  as the loss function during training,  $f$  and  $h$  are explicitly defined in [23] as

$$f = \arg \min_{f \in \mathcal{F}} \int_{\mathcal{X}} \int_{\mathcal{Y}} l(y, f(x)) P_{X,Y}(x, y) dy dx, \quad (10)$$

$$h = \arg \min_{h \in \mathcal{H}} \int_{\mathcal{X}} \int_{\mathcal{Y}} l(y, h(x)) P_{X,Y}(x, y) dy dx. \quad (11)$$

**Approximation Uncertainty** counts for the uncertainty due to the limited number of training samples. Assuming we have  $N$  samples available, the definition of  $\hat{h}$  is listed as

$$\hat{h} = \arg \min_{h \in \mathcal{H}} \frac{1}{N} \sum_{i=1}^N l(y_i, h(x_i)). \quad (12)$$

It is obvious that, unlike aleatoric uncertainty, model uncertainty and approximation uncertainty are reducible by enlarging the function space  $\mathcal{H}$  and increasing sample size  $N$ . We recommend [40]–[42] for the latest progress in predicting, sampling, and quantifying epistemic uncertainty.

#### IV. METHODS FOR UNCERTAINTY REPRESENTATION

In the realm of UQ, Bayesian methods stand as a pivotal approach, offering a powerful framework for representing uncertainty. At the heart of Bayesian UQ is the application of *Bayes' Theorem*, which provides a mathematical framework for updating our knowledge about a parameter  $\theta$  when we observe new data  $D$ . The theorem combines prior probability  $P(\theta)$  with the likelihood  $P(D|\theta)$  to produce the posterior probability  $P(\theta|D)$ , normalized by the marginal likelihood  $P(D)$ :

$$P(\theta|D) = \frac{P(D|\theta)P(\theta)}{P(D)}. \quad (13)$$

Advancing from the foundational Bayesian principles, we delve into three distinct categories methods for uncertainty representation in graph learning: direct inference, Bayesian representation learning, and Gaussian Processes.

##### A. Direct Inference

Direct inference is well-suited for semi-supervised node classification on graphs because a node's neighboring nodes can be treated as new observed data, or *evidence*, allowing for direct updates to the node's classification. One approach that directly applies Bayesian methods to infer the posterior probability distribution of nodes is as follows: First, a prior probability distribution is assigned to each node, which is then updated with evidence propagated from other nodes to obtain the posterior distribution. In [43], the node label is modeled as a categorical random variable as  $P(\hat{y}_i = k|\theta)$ , where  $\hat{y}_i$  is the predicted label of a node and  $\theta$  is the parameter of the categorical distribution. Based on the assumption that connected nodes are likely to share a label, it is assumed that a neighbor of a node shares the same parameter  $\theta$  as the node itself. For a node  $i$ , this leads to the multinomial likelihood function for the labels of its neighbors:  $P(\hat{N}_i|\theta) \propto \prod_{k=1}^K \theta_k^{n_{ik}}$ , where  $\hat{N}_i$  represents the set of labeled neighbors of node  $i$ , and  $n_{ik}$  is the number of neighbors of node  $i$  with label  $k$ . The corresponding conjugate Dirichlet prior for the parameter  $\theta$  is given by:  $P(\theta) \propto \prod_{k=1}^K \theta_k^{\alpha_k - 1}$ , where  $\alpha = (\alpha_1, \alpha_2, \dots, \alpha_K)^T$  is the parameter of Dirichlet distribution. By combining these, the posterior distribution of  $\theta$  is:  $P(\theta|\hat{N}_i) \propto \prod_{k=1}^K \theta_k^{\alpha_k + n_{ik} - 1}$ .

Beyond this label-sharing assumption and label propagation, [44] introduced the propagation of multinomial messages to support both homophily and heterophily network effects. This

was achieved by using compatibility matrices to represent the strength of connections between nodes. To handle high-dimensional features of nodes, [45] employed MLP encoding to compute node-level pseudo-counts, and then propagated them via PPR-based message passing. All three methods utilize Dirichlet priors and posteriors, with the main difference being the form of the evidence  $n_{ik}$  that is propagated.

##### B. Bayesian Representation Learning

###### 1) Bayesian Representation Learning Overview:

Representation learning refers to the process of automatically learning meaningful and useful features or representations from raw data, typically through models like neural networks. The goal is to transform the data into a format that captures the underlying structure or patterns, making it more suitable for machine learning algorithms to process and extract insights. Unlike traditional deterministic methods, Bayesian representation learning models the uncertainty of both model parameters and learned representations, treating them as random variables with associated probability distributions instead of fixed values. In this survey, we focus on two prominent classes of Bayesian representation learning: variational autoencoders (VAEs) [46] and Bayesian neural networks (BNNs) [47], [48].

**VAEs.** Autoencoders typically consist of two main components: an encoder and a decoder. The encoder, often denoted by a function such as  $f_\phi(\mathbf{x})$ , maps the input data  $\mathbf{x}$  deterministically into a latent representation  $\mathbf{z}$ . The decoder, denoted by  $g_\theta(\mathbf{z})$ , then seeks to reconstruct the input data from this latent representation. The aim is to minimize the reconstruction error, typically measured by a loss function such as mean squared error for continuous input data or cross-entropy loss for binary input data. While traditional autoencoders output a fixed latent representation  $\mathbf{z}$ , VAEs extend this framework by introducing a variational encoder. This encoder learns the parameters of a probability distribution over the latent space, allowing  $\mathbf{z}$  to be sampled from this distribution, thereby capturing the uncertainty in the representation.

A key technique in VAEs involves approximating the intractable posterior distribution  $p_\theta(\mathbf{z}|\mathbf{x})$  using a simpler distribution  $q_\phi(\mathbf{z}|\mathbf{x})$ . To achieve this, the Evidence Lower Bound (ELBO) is maximized [46]:

$$\mathcal{L}_{\text{ELBO}}(\theta, \phi; \mathbf{x}) = \mathbb{E}_{q_\phi(\mathbf{z}|\mathbf{x})} [\log p_\theta(\mathbf{x}|\mathbf{z})] - \text{KL}[q_\phi(\mathbf{z}|\mathbf{x}) \| p_\theta(\mathbf{z})]. \quad (14)$$

The first term is the expected log-likelihood and the second term is the KL divergence between the encoder's distribution  $q_\phi(\mathbf{z}|\mathbf{x})$  and  $p_\theta(\mathbf{z})$ , the prior distribution over the latent variables. VAEs capture uncertainty in the data by modeling the latent variables as distributions rather than fixed points. The variance of  $q_\phi(\mathbf{z}|\mathbf{x})$  reflects this uncertainty. The KL divergence term in the ELBO balances fitting the data accurately while maintaining a prior over the latent space, embedding a principled approach to UQ in representation learning.

**BNNs.** Bayesian Neural Networks (BNNs) integrates the flexibility of neural networks with the probabilistic rigor of Bayesian inference. BNNs assign probability distributions to the neural network's parameters  $\theta$ , which encapsulates model uncertainty. This is a departure from traditional neural

TABLE II  
TAXONOMY FOR UNCERTAINTY QUANTIFICATION METHODS

Purpose	Uncertainty Representation (Sec. IV)		Uncertainty Handling (Sec. V)		
Methodology	Bayesian✓ Direct Inference	Bayesian✓ Representation Learning	Calibration	Conformal Prediction	OOD Detection
Post-hoc			✓	✓	
Uncertain Parameter	✓	✓			
Distribution Free Input			✓	✓	✓
Regression Task	✓	✓		✓	✓
Classification Task	✓	✓	✓	✓	✓
Aleatoric and Epistemic Uncertainty Separation	✓	✓			
Accuracy Impact	✓	✓			✓
Back Propagation	✓	✓	✓		
Computational Cost	High	High	Low	Low	Low

networks that only yield a single point estimate of parameters. During training, BNNs use Bayesian inference to update the prior distribution  $P(\theta)$  with the likelihood  $P(D|\theta)$ , producing a posterior distribution that combines prior knowledge with observed data, as shown in Eq. (13). For predictions, BNNs leverage Bayesian model averaging, which involves integrating over the posterior distribution of the parameters to account for uncertainty. For a given test sample  $\mathbf{x}^*$ , the prediction thereby incorporates the model uncertainty, yielding the predictive distribution:

$$p(y^*|\mathbf{x}^*, D) = \int p(y^*|\mathbf{x}^*, \theta)p(\theta|D)d\theta. \quad (15)$$

Due to the general intractability of the integral, various techniques for inferring  $p(\theta|D)$  have been proposed. [49] demonstrated that Monte Carlo dropout is equivalent to sampling from an approximate posterior of  $\theta$ , allowing Eq. (15) to be simplified to the following Monte Carlo integral:

$$p(y^*|\mathbf{x}^*, D) \approx \frac{1}{S} \sum_{i=1}^S p(y^*|\mathbf{x}^*, \theta_i), \quad (16)$$

where dropout is used to obtain  $S$  weights  $\theta_i$ . Given the challenges associated with exact inference, another widely-used technique for approximating the posterior distribution  $p(\theta|D)$  is variational inference (VI). The objective is to approximate a distribution  $q_\phi(\theta)$  that is close to the posterior  $p(\theta|D)$ , which is also achieved by maximizing the ELBO.

## 2) Bayesian Representation Learning for Graphs:

The need to represent the complexity of graph-structured data while quantifying uncertainty has driven the development of Bayesian graph representation learning. Unlike deterministic embeddings that provide fixed representations, Bayesian graph representation learning captures the stochastic nature of graphs, accounting for irregular structures, noisy features, and other uncertainties to produce more faithful representations. GNNs lay the groundwork by leveraging local neighborhood information, but their deterministic nature often falls short in capturing the inherent uncertainty of real-world graphs. To address these limitations, two prominent approaches have been developed: graph variational autoencoders (GVAEs) and Bayesian graph neural networks (BGNNs).

**GVAEs.** [50] proposed a novel framework for unsupervised learning on graph-structured data using variational autoencoders. The GCN based encoder transforms the input graph  $G$  with nodes  $V$  into a latent space  $\mathbf{Z}$ , where each node  $i$  is mapped to a latent vector  $\mathbf{z}_i$ . The variational posterior  $q(\mathbf{Z}|\mathbf{X}, \mathbf{A})$  is approximated as a product of Gaussian distributions for each node. The model defines the posterior as  $q(\mathbf{z}_i|\mathbf{x}_i, \mathbf{A}) = \mathcal{N}(\mathbf{z}_i|\boldsymbol{\mu}_i, \text{diag}(\boldsymbol{\sigma}_i^2))$ , where  $\boldsymbol{\mu}$  and  $\log \boldsymbol{\sigma}^2$  are the outputs of a GCN applied to the graph's adjacency matrix  $\mathbf{A}$  and node features  $\mathbf{X}$ . The objective function derived from the ELBO (Eq. 14) to be optimized is

$$\mathcal{L} = \mathbb{E}_{q(\mathbf{Z}|\mathbf{X}, \mathbf{A})}[\log p(\mathbf{A}|\mathbf{Z})] - \text{KL}[q(\mathbf{Z}|\mathbf{X}, \mathbf{A})||p(\mathbf{Z})], \quad (17)$$

The term  $\log p(\mathbf{A}|\mathbf{Z})$  represents the reconstruction loss, which encourages the model to accurately reconstruct the graph's adjacency matrix. The KL divergence term  $\text{KL}[q(\mathbf{Z}|\mathbf{X}, \mathbf{A})||p(\mathbf{Z})]$  acts as a regularizer, ensuring that the learned distribution does not deviate too far from the prior  $p(\mathbf{Z})$ .

The model in [50], while effective, has several limitations, including insufficient modeling of graph dependencies, inability to explain latent factors, and inadequate handling of isolated nodes, various methods have been introduced. To address these issues, various methods have been developed.

[51] employed a hierarchical variational framework that enabled neighboring nodes to share information, thereby improving the modeling of the graph's dependency structure. This approach allowed the propagation of graph structural information and distribution uncertainty, which are essential for capturing complex posterior distributions. To clearly explain what latent factors are and why they perform well, [52] introduced the Dirichlet Graph Variational Autoencoder (DGVAE) with graph cluster memberships as latent factors. This study connects VAE-based graph generation with balanced graph cut, providing a new perspective on how to enhance the internal mechanisms of VAEs for graph generation. [53] observed that existing autoencoders produce embeddings for isolated nodes that are close to zero, regardless of their content features. To address this issue, [53] proposed a novel Variational Graph Normalized AutoEncoder (VGNAE) that utilizes  $L_2$ -normalization to derive improved embeddings for isolated nodes. [54] proposed an "iterative" GNN-based decoder to address the limitation of generating only node embeddings,

as this is not conducive to sampling new graphs. In contrast to the node-level VGAE described earlier, [55] proposed a graph-level VAE [56], named GraphVAE, which modifies the encoder and decoder functions to work with graph-level latent representations, consequently facilitating the direct modeling of uncertainty within graphs.

Capitalizing on the capabilities of graph variational autoencoders in representation and uncertainty modeling, several studies have incorporated them into GNNs for use in downstream tasks. [57] developed a novel hierarchical variational model that introduces additional latent random variables. This model jointly captures the hidden states of a Graph Recurrent Neural Network (GRNN) to effectively represent both topological changes and node attribute variations in dynamic graphs. To learn dynamic graph representations in hyperbolic space while also modeling uncertainty, [58] devised a hyperbolic graph variational autoencoder based on the proposed TGNN. This framework generates stochastic node representations from hyperbolic normal distributions.

**BGNNs.** Another route lies in transferring general Bayesian neural networks to GNNs. These works consider model parameters, passed messages, etc., as distributions rather than deterministic values, and propose a series of BGNNs. To address the inability of standard GCNs to model uncertainty in graph, [59] treated the observed graph  $G_{obs}$  as a sample from a random graph family. As a result, the posterior probability of node (or graph) labels can be computed by:

$$p(\mathbf{Z}|\mathbf{Y}_{\mathcal{L}}, \mathbf{X}, G_{obs}) = \int p(\mathbf{Z}|\boldsymbol{\theta}, G, \mathbf{X})p(\boldsymbol{\theta}|\mathbf{Y}_{\mathcal{L}}, G, \mathbf{X}) \cdot p(G|\lambda)p(\lambda|G_{obs}) d\boldsymbol{\theta} dG d\lambda. \quad (18)$$

Here  $\boldsymbol{\theta}$  is a random variable representing the parameters of a Bayesian GCN over graph  $G$ , and  $\lambda$  denotes the parameters that characterize a family of random graphs.  $\mathbf{Y}_{\mathcal{L}}$  and  $\mathbf{X}$  represent the training label set and the node feature matrix, respectively.  $p(\mathbf{Z}|\boldsymbol{\theta}, G, \mathbf{X})$  can be modeled using a categorical distribution by applying a softmax function to the output of the  $L$ -layer GCN  $\mathbf{Z} = \mathbf{H}^{(L)}$ . Due to the intractability of the integral in Eq. (18), the authors employ the following Monte Carlo approximation:

$$p(\mathbf{Z}|\mathbf{Y}_{\mathcal{L}}, \mathbf{X}, G_{obs}) \approx \frac{1}{N_G S} \sum_{i=1}^{N_G} \sum_{s=1}^S p(\mathbf{Z}|\boldsymbol{\theta}_{s,i}, G_i, \mathbf{X}). \quad (19)$$

In this approximation,  $N_G$  graphs  $G_i$  are sampled from  $p(G|\hat{\lambda})$ , where  $\hat{\lambda}$  is the parameter of the random graph model obtained through maximum a posteriori estimation  $\hat{\lambda} = \arg \max_{\lambda} p(\lambda|G_{obs})$ .  $S$  weights  $\boldsymbol{\theta}_{s,i}$  are drawn from  $p(\boldsymbol{\theta}_{s,i}|\mathbf{Y}_{\mathcal{L}}, G_i, \mathbf{X})$  using Monte Carlo dropout. For the random graph model in Eq. (18), [59] utilized an assortative mixed membership stochastic block model (a-MMSBM) [60], [61]. As an alternative, [62] proposed a node copying-based generative model, while [63] introduced a non-parametric posterior distribution to infer graph topology.

In addition to considering the observed graph as sampled from a random graph family, some studies also treat the inputs and other elements within the GNN as random variables, thereby adopting a Bayesian perspective to model uncertainty.

Specifically, in these approaches, different components of the GNN are assigned probability distributions. Bayesian inference techniques are then employed to estimate the uncertainty associated with these components.

To model the propagation of uncertainty in message-passing mechanisms, [64] treated messages as multivariate Gaussian variables and employed GNNs to predict their means. Recognizing that additional neighboring nodes provide more evidence and reduce uncertainty, [64] defined an uncertainty propagation mechanism in GNNs for predicting the covariance of Gaussian distributions, which is different from traditional message passing. The covariance ultimately provides the uncertainty of predictions. [65] viewed model parameters as random variables and then obtained both epistemic uncertainty and aleatoric uncertainty based on the uncertainty decomposition method in [66], [67]. Additionally, this work incorporates uncertainty from evidence theory, namely *vacuity* due to lack of evidence and *dissonance* due to conflicting evidence, offering a richer representation of uncertainty. [68] considered the adjacency matrix  $\mathbf{A}$  as a random variable. The prior distribution of the adjacency matrix  $\mathbf{A}$  is given by:

$$p(\mathbf{A}) = \prod_{ij} p(A_{ij}), \text{ with } p(A_{ij}) = \text{Bern}(A_{ij}|\rho_{ij}^o), \quad (20)$$

where  $\text{Bern}(A_{ij}|\rho_{ij}^o)$  is a Bernoulli distribution over  $\rho_{ij}^o$ . The variational posterior, which takes a form similar to the prior, is given by:

$$q_{\phi}(\mathbf{A}) = \prod_{ij} q_{\phi}(A_{ij}), \text{ with } q_{\phi}(A_{ij}) = \text{Bern}(A_{ij}|\rho_{ij}), \rho_{ij} > 0, \quad (21)$$

where  $\rho_{ij}$  are free parameters, and  $\phi = \{\rho_{ij}\}$ . By relaxing the discrete distribution to a continuous Concrete distribution [69], [70] and maximizing a ELBO, they are able to estimate the parameters  $\phi$  of the posterior  $q_{\phi}(\mathbf{A})$ . [33] considered probabilistic links, noise in node features, and modeling errors, treating node features, links between nodes, and model parameters as random variables. The model propagates aleatoric uncertainty to the output by defining mechanisms for the means and variances of node embeddings in GNNs, while epistemic uncertainty is estimated using MC dropout.

### C. Gaussian Process

#### 1) Gaussian Process Overview:

Gaussian Processes (GPs) are a widely-used class of non-parametric Bayesian models that have been widely used for uncertainty quantification in machine learning [71]. A GP is defined as a collection of random variables, any finite number of which have a joint Gaussian distribution. In the context of function approximation, a GP can be used as a prior distribution over the space of functions, denoted as:

$$f(\mathbf{x}) \sim \mathcal{GP}(m(\mathbf{x}), k(\mathbf{x}, \mathbf{x}')), \quad (22)$$

where  $m(\mathbf{x})$  is the mean function and  $k(\mathbf{x}, \mathbf{x}')$  is the covariance function or kernel. The mean function represents the expected value of the function at any input point, while the covariance function captures the similarity between pairs of input points and determines the smoothness of the functions sampled from the GP.

Given a set of observed data  $\mathcal{D} = (\mathbf{x}_i, y_i)_{i=1}^n$ , where  $\mathbf{x}_i$  are the input points and  $y_i$  are the corresponding target values, the posterior distribution is a GP with updated mean and covariance functions:

$$\mu(\mathbf{x}) = m(\mathbf{x}) + \mathbf{k}(\mathbf{x})^T (\mathbf{K} + \sigma_n^2 \mathbf{I})^{-1} (\mathbf{y} - \mathbf{m}) \quad (23)$$

$$\Sigma(\mathbf{x}, \mathbf{x}') = k(\mathbf{x}, \mathbf{x}') - \mathbf{k}(\mathbf{x})^T (\mathbf{K} + \sigma_n^2 \mathbf{I})^{-1} \mathbf{k}(\mathbf{x}') \quad (24)$$

where  $\mathbf{k}(\mathbf{x}) = [k(\mathbf{x}, \mathbf{x}_1), \dots, k(\mathbf{x}, \mathbf{x}_n)]^T$ ,  $\mathbf{K}$  is the covariance matrix (or kernel matrix) with entries  $\mathbf{K}_{ij} = k(\mathbf{x}_i, \mathbf{x}_j)$ ,  $\mathbf{y} = [y_1, \dots, y_n]^T$ ,  $\mathbf{m} = [m(\mathbf{x}_1), \dots, m(\mathbf{x}_n)]^T$ , and  $\sigma_n^2$  is the noise variance.

The posterior distribution allows for uncertainty quantification in predictions. For a new input point  $\mathbf{x}_*$ , the predictive distribution is given by:

$$p(f_* | \mathbf{x}_*, \mathcal{D}) = \mathcal{N}(f_* | \mu(\mathbf{x}_*), \Sigma(\mathbf{x}_*, \mathbf{x}_*)). \quad (25)$$

The predictive mean  $\mu(\mathbf{x}_*)$  provides the expected value of the function at  $\mathbf{x}_*$ , while the predictive variance  $\Sigma(\mathbf{x}_*, \mathbf{x}_*)$  quantifies the uncertainty associated with the prediction.

One limitation of standard GPs is their computational complexity, which scales cubically with the number of training points due to the inversion of the covariance matrix. Various approximation techniques have been proposed to overcome this limitation [72]–[74], with the added benefit of enabling efficient UQ in GPs. Recent advancements have also explored the integration of GPs with deep learning architectures to leverage the strengths of both approaches [75], [76]. This integration enhances the ability to quantify uncertainty in complex and hierarchical data representations.

## 2) Gaussian Process for Graphs:

Applying GPs to graph-structured data has emerged as an important research direction in recent years [77]–[86]. This approach combines the powerful UQ capabilities of GPs with the complex structures of graph data, offering new possibilities for uncertainty estimation in graph learning tasks. This section focuses on works that are closely related to UQ in graph learning, while also introducing other relevant GP methods.

**Closely Related to UQ.** [77] were among the first to propose a Graph Gaussian Process (GGP) based semi-supervised learning method. This method can achieve good generalization performance even with limited labeled data, bridging the gap between simple models and data-intensive graph neural networks. GGP defines a GP prior over node embeddings, using a kernel function that can be selected from existing well-studied options. The model combines the GP prior with a robust-max likelihood [87] to handle multi-class problems. Since the posterior distribution is not analytically tractable, a variational inference-based approximation method with inducing points is used, similar to the inter-domain inference algorithm [88].

[78] proposed Uncertainty aware Graph Gaussian Process (UaGGP), an extension of the GGP model. UaGGP addresses the uncertainty in graph structures that may arise in semi-supervised learning problems on graphs, where edges can connect data points with different labels, leading to uncertainty in predictions. UaGGP uses GP to guide the model learning by

incorporating prediction uncertainty and label smoothness regularization. For any two nodes  $v_i$  and  $v_j$  in the graph, UaGGP defines an uncertainty-aware distance measure  $d(v_i, v_j)$  to constrain the proximity of their prediction results. When the model is not confident in the inference of  $v_i$  or  $v_j$  or both of them, the distance  $d(v_i, v_j)$  should not be small.

To detect potential failures of GNNs on OOD samples in the task of energy and force predictions on molecules, [84] proposed a method called Localized Neural Kernel (LNK) to address the uncertainty estimation problem in molecular force fields. LNK leverages GNNs as encoders within a Deep Kernel Learning framework and uses Sparse Variational Gaussian Processes (SVGP) to mitigate the computational burden associated with GPs. By directly fitting the GP on atomic embeddings, this method ensures the locality of uncertainty in predictions, particularly effective in modeling molecular interactions.

**Other GP Methods for Graph Learning.** [79] introduced GPGC, a GP regression model using GCNs that enhances expressive power by focusing on 1-hop neighborhood nodes with equal weights. [80] incorporated graph structures into the GP kernel using spectral graph wavelets, adopting a multi-scale approach to capture various levels of smoothness and adapt to different frequencies. Similarly, [81] proposed the GPG model, integrating the graph Laplacian into the GP covariance matrix to enhance spectral regularization of target signals in node regression tasks.

To address scalability in large-scale graph data, [82] developed Stochastic Deep Gaussian Processes over Graphs (DGGP), which leverages deep GPs to model complex mappings efficiently. In the context of graph classification, [83] introduced two models, FT-GP and WT-GP, utilizing graph Fourier and wavelet transforms to extract spectral features suitable for the GP framework, capturing multi-scale and localized patterns in graphs.

For link prediction, [85] proposed a graph convolutional variational GP model that combines graph convolution operations with GP to effectively utilize graph structures and node features. Lastly, [86] introduced the Multi-Relational GGPN, which employs GPs to model distributed embedding functions, allowing for the learning of a family of embedding functions and enhancing the model’s flexibility.

## V. METHODS FOR UNCERTAINTY HANDLING

### A. Out of Distribution

Out-of-distribution (OOD) refers to instances that significantly differ from a model’s training data. It is especially crucial for models in real-world applications that face unpredictable and uncertain inputs, in stark contrast to the controlled and uniform datasets used for training. When a model encounters OOD data, its *epistemic* uncertainty typically increases. OOD data typically lead to the model’s underperformance or unpredictable behavior because of its great difference from the training data, resulting in high prediction uncertainties. To address this problem, a surge of research has focused on out-of-distribution (OOD) generalization. Strategies to mitigate uncertainty issues posed by OOD generalization can be broadly classified into several categories [89], including distributionally robust optimization (DRO) [90]–[103], adversarial

training (AT) [104]–[106], and self-supervised learning (SSL) [107]–[110]. Most of them propose novel frameworks, network architectures, and objective functions to improve the model performance of OOD data during testing. However, this survey focuses on the measurement, calibration, and conformity of predictive uncertainty; thus, we will emphasize the integration of OOD and uncertainty studies, especially how to measure and estimate the disagreement between training and test data.

#### 1) Distributionally Robust Optimization:

Distributionally Robust Optimization (DRO) aims to enhance the model’s performance across a wide range of potential testing data distributions, instead of the training data distribution only. Specifically, DRO optimizes the objective function in the “worst case” of the distributions where the loss will be maximized. Formally, DRO is formulated by a bi-level optimization problem:

$$\min_{f \in \mathcal{F}} \max_{P \in \mathcal{P}} \mathbb{E}_{x \sim P} [\mathcal{L}_0(f, x)], \quad (26)$$

where  $\mathcal{L}_0$  is a classification loss, such as cross-entropy. The uncertainty set  $\mathcal{P} := \{P | D(P, P_0) \leq \rho\}$  includes all the data distributions  $P$  within the radius distance  $\rho$  from the observed data distribution  $P_0$ . The distance between two distributions is measured by  $D(\cdot, \cdot)$ , and we list the following choices of  $D$  used in DRO.

- **f-divergence**, also known as phi-divergence, is defined by  $D_f(P||P_0) := \int f\left(\frac{dP}{dP_0}\right) dP_0$ . It is widely used to quantify the divergence between the distributions in DRO [90]–[92]. The domain delineated by  $f$ -divergence can be viewed as a statistical confidence region, and the inner maximization problem in Eq. (26) is tractable for several choices of  $f$  [92], [93].
- **KL-divergence**, one special case of  $f$ -divergence, is used as a distance metric in DRO [94], [95]. However, the possible limitations of metrics based on  $f$ -divergence are that they may not be comprehensive enough to include some relevant distributions, or they may fail to precisely measure the distance for extreme distributions [96].
- Alternatively, **Wasserstein distance** alleviates the above limitations and is adopted to evaluate the distribution distance [96]–[101]. Formally, it is defined by  $D_W(P, P_0) := \inf_{\gamma \in T(P, P_0)} \int \int \gamma(p, q) c(p, q) dp dq$ , where  $T(P, P_0)$  contains all possible couplings of  $P$  and  $P_0$ , and  $c(p, q) \geq 0$  are some cost functions transferring from  $p$  to  $q$ . The authors in [100], [101] address data uncertainty by establishing an uncertainty set for the distributions of the observed data. Based on different assumptions on the uncertainty of the data, a graph learning framework employing Wasserstein DRO is proposed [100]. In [101], nodes of the same class are supposed to adhere to the underlying distribution within an uncertainty set, and the uncertainty set for each label is defined by the Wasserstein distance.
- Besides that, authors in [102] study DRO with uncertainty sets defined by **maximum mean discrepancy**. The authors in [103] propose to define the uncertainty sets using the **Prohorov metric**.

#### 2) Adversarial Training and Self-Supervised Learning:

Besides DRO, adversarial training (AT) and self-supervised learning (SSL) are proposed to mitigate OOD problems. However, most of the existing work adopts the  $L_p$ -norm or predefined perturbations to quantify or mimic the uncertainty.

In essence, AT on graphs addresses the following min-max optimization problem:

$$\min_{\theta} \max_{\|\epsilon_{\theta}\| \leq \rho_{\theta}, \|\epsilon_x\| \leq \rho_x, \|\epsilon_a\| \leq \rho_a} \mathcal{L}_0(\theta + \epsilon_{\theta}, X + \epsilon_x, A + \epsilon_a), \quad (27)$$

where  $\epsilon_{\theta}$ ,  $\epsilon_x$ , and  $\epsilon_a$  represent the perturbations applied to model parameters  $\theta$ , input node features  $X$ , and adjacency matrix  $A$ , respectively.  $\rho_{\theta}$ ,  $\rho_x$  and  $\rho_a$  ensures the perturbations  $\epsilon_{\theta}$ ,  $\epsilon_x$ , and  $\epsilon_a$  to be small enough and neglectable, respectively. Notice that the perturbation magnitude (uncertainty) is typically measured using the  $L_p$ -norm, such as the  $L_1$ ,  $L_2$ , or  $L_{\infty}$  norm, regardless of whether the input data [104], [106] or the model parameters [105], [106] are being perturbed.

The idea of SSL on graphs is to deliberate perturbation or modification of graphs to construct a new controllable dataset in which the intrinsic information of the graphs remains unchanged. The modifications are typically predefined and explicitly formulated, thus these works *cannot* provide precise measurements for changes (uncertainty). To facilitate the generation of positive pair instances, these works encompass augmentations such as node masking [107], edge perturbation, attribute masking, subgraph sampling [108], random walks for graph sampling [109], and both structural and attribute levels augmentations [110].

### B. Conformal Prediction

#### 1) Conformal Prediction Overview:

Conformal Prediction (CP) is an uncertainty quantification framework. For a given model and a predefined significant level  $\alpha$ , CP uses the calibration data to estimate the confidence intervals of predicted outcomes based on score functions [111]. In this section, we focus on CP for classification tasks, as GNN-related tasks inherently fall into this category.

**Inductive CP**, or called split conformal prediction (SCP), is a widely applied version of CP. For a trained classifier  $f$  and input  $x$  with label space  $\{1, 2, \dots, K\}$ , the estimated probability for each class is  $\hat{y} = f(x) \in [0, 1]^K$ . Let  $f(x)_y$  denote the true class from the final softmax layer. The calibration set  $D_{cal} = \{(X_i, Y_i)\}_{i=1}^n$  is applied to quantify how uncertain the model  $f$  would be. The score function  $s(x, y) = 1 - f(x)_y$  is widely selected for classification tasks, and it measures how predictions conform to the true values at inputs. The conformal score for  $(X_i, Y_i) \in D_{cal}$  is defined as  $s_i = 1 - f(X_i)_{Y_i}$ . Let  $S = \{s_i\}_{i=1}^n$ , the empirical quantile of  $S$  is given by

$$Q_{1-\alpha}(S) = \lceil (1 - \alpha)(n + 1) \rceil / n\text{-th quantile of } S. \quad (28)$$

If a test sample  $(X_{n+1}, Y_{n+1})$  drawn exchangeably with the elements of  $D_{cal}$ , we apply CP to construct a prediction set  $C(X_{n+1}) = \{k | 1 - f(X_{n+1})_k \leq Q_{1-\alpha}\}$ , which includes all classes  $k \in \{1, \dots, K\}$  whose conformal score is less or equal to  $Q_{1-\alpha}$ . Under the assumption of exchangeability, the coverage guarantee holds that

$$\Pr(Y_{n+1} \in C(X_{n+1})) \geq 1 - \alpha. \quad (29)$$



**Transductive CP**, also referred to as full conformal prediction (FCP), is the first proposed method for conducting CP [111]. With training data  $D_{train} = \{(X_i, Y_i)\}_{i=1}^n$  and a test input  $X_{n+1}$ , the trained model  $f^k$  is based on  $D_{train} \cup \{(X_{n+1}, k)\}$ ,  $\forall k \in \{1, 2, \dots, K\}$ , so multiple models need to be trained. For each  $f^k$ , the conformal scores are  $s_i^k = 1 - f^k(X_i)_{Y_i}$  and  $s_{n+1}^k = 1 - f^k(X_{n+1})_k$ . If  $s_{n+1}^k$  is less than the  $1 - \alpha$  quantile of  $\{s_i^k\}_{i=1}^n$ , we put the corresponding  $k$  to the prediction set of  $X_{n+1}$ .

To make the size of  $C(X_{n+1})$  more adaptive to  $X_{n+1}$  under the exchangeability assumption, novel conformal score functions are proposed, such as [112]–[115]. However, the exchangeability assumption can be violated by distribution shift between calibration distribution  $P_{XY}$  and test distribution  $Q_{XY}$  such that  $(X_{n+1}, Y_{n+1})$  is **non-exchangeable** with the elements of  $D_{cal}$ . In the case of **covariant shift** ( $P_X \neq Q_X$ ), [116] introduces an importance weighting technique based on likelihood ratio to maintain the coverage guarantee in Eq.(29). When **concept shift** ( $P_{Y|X} \neq Q_{Y|X}$ ) occurs, the authors of [117], [118] focus on keeping  $1 - \alpha$  coverage on test data under dynamic shift with time, and the authors of [119]–[121] ensure the coverage guarantee on test data under stationary distribution shift (does not change with time). [122] bounds the coverage gap by the total variation distance between calibration and test conformal scores under the non-exchangeability condition.

## 2) Conformal Prediction for Graphs:

For node classification tasks on graphs, the exchangeability may be violated for some specific settings [123]. First, in the *transductive* settings, the model has access to the entire graph structure and all the node features during training, calibration, and testing, but the labels of calibration and testing set are not available during training. In this case, the union of calibration and the unlabeled sample is exchangeable. However, in the *inductive* settings, the model only has access to the subgraph induced by the nodes in the training set  $D_{train}$  during training. The assumption of exchangeability does not hold in this case.

The authors in [124] adopt the jackknife method to estimate the uncertainty of a node  $X_i$  inferred by a GNN. Specifically, uncertainty  $\mathbb{U}(X_i) = \mathbb{C}^+(X_i) - \mathbb{C}^-(X_i)$  is the difference between the lower and upper bound of the predictive confidence interval. Both bounds are defined by leave-one-out (LOO) loss, which are approximated by the influence function.

Another branch of research proposes new score functions for CP on graphs. The diffused adaptive prediction sets (DAPS) is introduced in [123]. DAPS exploits the graph structure based on neighborhood diffusion, and defines the diffused score as

$$\hat{s}(X_i, Y_i) = (1 - \lambda)s(X_i, Y_i) + \frac{\lambda}{|\mathcal{N}_i|} \sum_{X_j \in \mathcal{N}_i} s(X_j, Y_i), \quad (30)$$

where  $\lambda$  signifies the diffusion parameter. Note that the diffused score function preserves exchangeability if the original scores are exchangeable. This diffusion process proves particularly advantageous in homophilous graphs, where connected nodes exhibit similar ground truth distributions. The rationale behind this is that for a node surrounded by mostly unperturbed neighbors, its probability can be better estimated

using its neighbors' information, as long as these vectors are sufficiently similar.

For the non-exchangeable conformal prediction cases, the procedure assumes a choice of deterministic fixed weights  $w_1, \dots, w_n \in [0, 1]$  [122]. Then the prediction set concerning the weighted quantiles of the score distribution is

$$\hat{C}(X) = \left\{ Y \in \mathcal{Y} : s(X, Y) \leq Q_{1-\alpha} \left( \sum_{i=1}^n w_i \delta_{s_i} \right) \right\}, \quad (31)$$

where  $Q_{1-\alpha}$ , as defined in Eq. (28), is the  $(1 - \alpha)$ -quantile of a distribution. The inductive cases are studied in [125], where the principle of exchangeability is not applicable. Based on the adaptive prediction set (APS) [112], they integrate non-exchangeable conformal prediction with the concept of homophily in graphs, leading to three distinct variants of the neighborhood adaptive prediction sets (NAPS) for the prediction set construction. The primary variant, NAPS, assigns the weights in Eq. (31) to  $w_i = 1$  if  $X_i \in \mathcal{N}_{n+1}^K$ , where  $\mathcal{N}_{n+1}^K$  includes all nodes within  $K$ -hop neighborhood of node  $X_{n+1}$ . The second one, NAPS-H, adopts a hyperbolic decay rate for  $w_i = k^{-1}$  where  $k$  is the  $k$ -hop neighbor of node  $X_{n+1}$ . The third one, NAPS-G, uses a geometric decay rate for  $w_i = 2^{-k}$ .

## C. Calibration

### 1) Calibration Overview:

Machine learning models on classification tasks are expected to output predicted labels with reliable confidence. For example, for a prediction with confidence = 0.8, its probability of correctness is expected to be 80% as well.

**Calibration Formulation.** We begin with a classifier  $f$  trained by a feature set and a corresponding label set whose label space is  $\mathcal{Y} = \{1, \dots, K\}$ . With inputs  $x_i$  and the true label  $y_i$  as an one-hot vector  $\mathbf{y}_i = (y_i^1, \dots, y_i^K)$  for  $i = 1, \dots, n$ ,  $f$  applies softmax operation to output a probability vector,  $\mathbf{v}_i = (v_i^1, \dots, v_i^K)$ ,  $\sum_{j=1}^K v_i^j = 1$ . The predicted label and confidence of  $x_i$ , denoted by  $\hat{y}_i$  and  $\hat{p}_i$  respectively, are

$$\hat{y}_i = \arg \max_{j \in \mathcal{Y}} v_i^j, \quad \hat{p}_i = \max_{j \in \mathcal{Y}} v_i^j. \quad (32)$$

A model is well-calibrated if the probability of correct prediction equals the prediction confidence for all labels and all confidence levels [9], or more formally,  $\Pr(y_i = j | v_i^j = p) = p$ ,  $\forall j \in \mathcal{Y}$ ,  $\forall p \in [0, 1]$ .

**Calibration Method.** Calibration can be conducted on top of accuracy-driven models, called post-processed methods. Histogram binning is initially proposed in [126] as a non-parametric calibration method. For a binary classification task with label space  $\mathcal{Y} = \{0, 1\}$  and  $\hat{p}_{i,1}$  as the confidence of input  $x_i$  in label 1,  $B_m$  is a set including samples whose  $\hat{p}_{i,1}$  is in the interval  $I_m = (\frac{m-1}{M}, \frac{m}{M}]$  based on user-defined  $M$ , so we can use a calibration set to minimize

$$\min_{\theta_1, \dots, \theta_M} \sum_{m=1}^M \sum_{i \in B_m} (\theta_m - y_i)^2, \quad (33)$$

where  $\theta_m$  is the estimated number of positive-class samples in the  $B_m$  set. For a test sample  $x_{n+1}$  whose  $\hat{p}_{n+1,1}$  belong

to  $I_m$ ,  $\hat{p}_{n+1,1}$  should be replaced by  $\theta_m$  as a calibrated confidence. As Isotonic regression in [127] suggested, the number and size of  $I_m$  can also be optimized. [128] applied isotonic regression to deep learning models for regression tasks with promising performance. Both histogram binning and isotonic regression can be applied to multi-class classification tasks using the one-vs-rest strategy. Platt scaling is a parametric calibration method introduced in [129]. Traditionally,  $\mathbf{v}_i$  is transformed from a logit vector  $\mathbf{z}_i$  via softmax function  $\sigma(\cdot)$ . Platt scaling generalizes the process by  $\mathbf{v}_i = \sigma(\mathbf{W} \cdot \mathbf{z}_i + \mathbf{b})$ , which can be optimized by minimizing negative log-likelihood on a calibration set. When  $\mathbf{W}$  is a scaler and  $\mathbf{b} = 0$ , it is also referred to as temperature scaling.

Calibration can also be conducted during the training phase, without requiring an additional calibration dataset. Traditionally, we train a model with cross-entropy (CE), which is equivalent to NLL loss when we use a softmax output layer in a multi-class classification problem and encode labels as one-hot vectors. However, CE and NLL are minimized when a model assigns a high probability to the correct class for each instance. In other words, a model is rewarded for being overconfident in its correct predictions, and miscalibration can be caused by the overfitting of CE loss and NLL loss [130], [131]. To mitigate the issue, label smoothing tunes a parameter  $\alpha \in [0, 1]$ , so the one-hot vector  $\mathbf{y}_i = (y_i^1, \dots, y_i^K)$  becomes smoother by

$$\mathbf{y}_i \rightarrow \mathbf{y}'_i = \left( (1 - \alpha)y_i^1 + \frac{\alpha}{K}, \dots, (1 - \alpha)y_i^K + \frac{\alpha}{K} \right), \quad (34)$$

so it penalizes the model for assigning a full probability to the ground truth label [132]. Similarly, focal loss (FL) is introduced in [133] and it is applied to calibration in [131] with the loss function:

$$\text{FL}(x_i) = -(1 - \hat{p}_i)^\gamma \log(\hat{p}_i), \gamma \geq 0. \quad (35)$$

Focal loss only considers confidence in the true label and the loss value will decrease faster as we increase  $\gamma$ , so it can prevent being over-confident. If  $\gamma = 0$ , FL goes back to CE.

## 2) Calibration for Graphs:

Accuracy alone is not enough for high-stake decision-making. The calibration performance of modern neural networks has been proven poor along a series of factors, including network width, depth, batch normalization, and weight decay [9]. Calibration on GNNs also started to draw people's attention recently as well. GNNs for classification tasks can generate softmax outputs that can be regarded as probabilities that the predicted results are correct.

**Node-level Classification.** Traditional calibration techniques are typically applied to models handling independent and identically distributed (i.i.d.) data. In contrast, graph data, or relational data, presents a unique challenge due to its dependent nature. In graph data, the characteristics or status of one node may be influenced by the attributes or conditions of neighboring nodes, highlighting an inherent dependency where a node's properties are not solely its own but also a reflection of its position within the graph [134]. This interdependency complicates the calibration process for GNNs. Furthermore, issues with class imbalance can lead to collapsed predictions,

necessitating the adjustment of class weights during the training phase.

The calibration performance of GNNs on node-level classification tasks is related to GNNs' architectures, neighbors' labels, and the number of training epochs. The authors of [135], [136] validate the general tendency towards underconfidence for predictions of GNNs. Besides, it is proved that GNNs with wider layers tend to be better calibrated, and GNNs change from being under-confident to overconfident as the number of network layers increases [137], [138]. Calibration error on the classification of a node can be influenced by the node's neighbor as well. Experimental results of [135], [136] show that calibration error decreases and a node tends to have similar confidences with its neighbors when more neighbors have the same label as the center one. However, the results of [137] reveal that well-calibration is more likely to occur when the same-class-neighbor ratio is around 0.4 to 0.5. Even though both results are drawn from GCN with the same datasets, the conflicts are probably caused by the different network structures and numbers of training epochs. As the experiments in [137] demonstrate, GNNs tend to be under-confident with early stopping and will be overconfident with too many training epochs, as they start to overfit training data.

Conventional calibration methods can not recalibrate GNNs well. Compared with Monte-Carlo dropout (MC-dropout) [49], histogram binning [126], and isotonic regression [127], temperature scaling (TS) [129], [139] usually outputs the best calibration results in the experiment of [134]. Similarly, experiments in [140] validate that the overall performance of Platt scaling (PS), TS, Accuracy-versus-Uncertainty (AvU) [141], and Graph Calibration Loss (GCL) [138], which will be introduced soon, is better than MC-dropout and Model Ensemble [142] techniques. Since MC-dropout and Model Ensemble rely on averaging predictions from multiple models, the limited architectural diversity of GCNs may cause their underperformance. Moreover, the authors of [140] find out models optimized on multi-class node classification tasks will be better calibrated and more discriminative than those trained on binary classification tasks.

The calibration methods for GNNs can be post-processed. CaGCN is a topology-aware post-hoc calibration GCN model developed in [135] assuming that neighboring nodes share similar ground truth confidence levels with the center one. With an undirected attributed GCN optimized for prediction accuracy, CaGCN works as another GCN to calibrate the outputs of the accuracy-driven model, thus it can be regarded as a Platt scaling method adapted to graphic models. To preserve the accuracy of the original classification GCN, the optimization objective function of CaGCN is a combination of negative log-likelihood loss and a customized calibration loss on validation nodes with a balancing hyperparameter. Graph Attention Temperature Scaling (GATS) [136] is also a post hoc method, and embeds the attention mechanism for node-wise calibration. For each node, a scaling process will consider global calibration bias, relative confidence compared with neighbors, and aggregated neighborhood influence with corresponding attention coefficients. Ratio-binned scaling (RBS),

proposed in [137], follows the logic of histogram binning to calibrate outputs of a GNN. RBS will first estimate the same-class-neighbor ratio of each node, group them into  $M$  bins, and finally learn a temperature for each bin to re-calibrate them.

Conducting calibration during model training is also attractive since it does not require additional data and computation costs. Graph Calibration Loss (GCL) is introduced in [138] as an end-to-end calibration method for GNNs. GCL is designed to minimize the discrepancy between the ground-truth probability distribution  $p$  and predicted confidence distribution  $\hat{p}$ . Specifically, GCL is the KL divergence between  $p$  and  $\hat{p}$  regularized by the product of their entropy. HyperU-GCN is proposed in [143] to calibrate the hyperparameter uncertainty of automated GNNs by defining it as a bi-level problem. The upper-level problem explains uncertainties by developing probabilistic hypernetworks through a variational Bayesian method. The lower-level problem learns how hyperparameter distribution is propagated to GCN weights.

To make GNNs robust to adversarial attacks and discriminatory biases, FairGNN [144], RobustGNN [145], and NIFTY [146] are proposed to enhance the stability of GNNs. However, these methods will make GNNs either overconfident in incorrect predictions or biased to global graph noises. To address the problem, Multi-view Confidence-calibrated NIFTY (MCCNIFTY) is introduced in [147]. Based on evidential theory, a novel node embedding learning module is developed. It includes an intra-view evidence calibration, an inter-view evidence fusion, and an uncertainty-aware message-passing process, optimizing for counterfactual fairness and stability at the sub-graph level.

**Link Prediction.** An important downstream task for GNN node classification is link prediction [148]. The authors of [149] study the calibration performance of link prediction and find that GNNs tend to be overconfident in negative link predictions but underconfident in positive ones. To address the issue, IN-N-OUT is proposed to parameterize a temperature for calibration. Two embeddings of an edge will be obtained when training the GNNs with and without the edge, and calculating the discrepancy between the two embeddings of the edge will help determine the value of temperature scaling.

Anchoring technique, named as  $\Delta$ -UQ, is introduced in [150] to estimate the uncertainty of predictions. During training, an anchor  $c$  is randomly chosen for stochastic centering, and a relative representation  $[x - c, c]$  of each input  $x$  is created. The anchor value is different in each training iteration. For inference,  $\Delta$ -UQ collects multiple predictions of an input  $x$  with different predefined  $c$  and estimates uncertainty based on aggregated predictions.

The anchoring technique is adopted in [151] to calibrate the prediction uncertainty for link prediction. It defines link prediction by two processes: passing node information with a multi-layer deterministic encoder and predicting the label of two nodes with a stochastic decoder. The proposed method is named as E- $\Delta$ UQ with three variants. The first variant applies anchoring between encoding and decoding, thus it is based on deterministic node features. The second variant implements one more anchoring after specific layers of encoding. Based

on the second one, the last variant pre-trains the encoder with an auxiliary attribute masking task on node features.

**Graph-level Classification.** The anchoring technique is also adopted in [152], named as G- $\Delta$ UQ with three variants, for the calibration of GNNs on graph-level classification tasks under the conditions of covariate and concept shifts using Superpixel-MNIST datasets [153]–[156]. The first variant is node feature anchoring, implemented when inputting training data. A Gaussian distribution is fitted to node features in training data and an anchor is randomly selected from the distribution for each node. The second variant is intermediate anchoring, which applies stochastic centering for each node after specified hidden layers. Readout anchoring is the last variant applying anchoring to the final graph representation before a graph-level readout function, instead of anchoring for each node.

## VI. UNCERTAINTY QUANTIFICATION EVALUATION

### A. Calibration

The evaluation of calibration measures the difference between a model's prediction confidence and the exact probability that the predicted output is correct. This section introduces two widely applied metrics.

**Expected Calibration Error (ECE).** We divide the entire confidence space  $[0,1]$  into  $M$  equal-size intervals  $I_m = (\frac{m-1}{M}, \frac{m}{M}]$  for  $m = 1, \dots, M$ .  $B_m$  is the set of samples with confidences in  $I_m$ . The accuracy and confidence of  $B_m$  are

$$\text{acc}(B_m) = \frac{1}{|B_m|} \sum_{i \in B_m} \mathbf{1}(\hat{y}_i = y_i), \quad (36)$$

$$\text{conf}(B_m) = \frac{1}{|B_m|} \sum_{i \in B_m} \hat{p}_i. \quad (37)$$

respectively, where  $y_i$  and  $\hat{y}_i$  are the true and predicted label of input  $x_i$ , and  $\hat{p}_i$  is the confidence of the prediction. Expected Calibration Error (ECE) computes the absolute difference between  $\text{acc}(B_m)$  and  $\text{conf}(B_m)$ :

$$\text{ECE} = \sum_{m=1}^M \frac{|B_m|}{n} |\text{acc}(B_m) - \text{conf}(B_m)|. \quad (38)$$

A reliability diagram can be plotted with  $\text{acc}(B_m)$  and  $\text{conf}(B_m)$  to visualize a model's calibration performance [157]. The plot of a well-calibrated model should follow a diagonal, indicating the accuracy is the same as confidence. Some works extend the concept of ECE to make it suitable for different scenarios. For example, Maximum Calibration Error (MCE) computes the maximum gap between accuracy and confidence for  $m = 1, \dots, M$  [158], and Class-wise ECE (cwECE) is designed to see averaged ECE on class level [159].

To evaluate the calibration of node-level classification models on GNNs, node-wise ECE follows the concept of ECE. Specifically, test nodes are partitioned into bins according to their prediction confidences, and nodewise-ECE works as Eq. (38) to quantify the summation of the absolute difference between confidence and accuracy across all bins [134], [135], [137], [138]. However, nodewise-ECE neglects graph structure and the interdependencies between nodes. To remedy this,

edge-wise ECE is proposed in [160]. With graph  $G = (\mathcal{N}, \mathcal{E})$ , denote  $\mathcal{E}_U = \{(i, j) \in \mathcal{E} | i, j \in U\}$  the subset of edges  $\mathcal{E}$  constrained to test nodes  $U$ . The confidence of edge  $(i, j)$  is  $\hat{c}(i, j) = \max_{l, m} \hat{p}(y_i = l, y_j = m)$ , given the features of all nodes and labels of training nodes. The calculation of edge-wise ECE is similar to node-wise ones. Specifically, each  $\hat{c}(i, j)$  is computed and assigned to corresponding bins, and a prediction is considered accurate only if both predicted  $l$  and  $m$  are correct. The summed gap between confidence bins and accuracy is edge-wise ECE, similar to Eq. (38). Additionally, ECE for agreeing node pairs and disagreeing node pairs are also proposed [160].

**Proper Scoring Rules.** As ECE depends on the resolution of the finite number of bins, a continuous proper scoring rule, such as Brier Score (BS) [161], can act as an alternative to ECE. Brier Score (BS) considers a sample's confidence in all labels. It is given by

$$\text{BS} = \frac{1}{n} \sum_{i=1}^n \sum_{j=1}^K (\hat{p}_{i,j} - \mathbb{1}(y_i = j)), \quad (39)$$

where  $\hat{p}_{i,j}$  is the confidence of sample  $i$  in label  $j$ . A lower Brier Score indicates not only that a model is well-calibrated but also that the model is confident in its predictions.

### B. Conformal Prediction

**Conditional Coverage Metric.** The key contribution of conformal prediction is stated in Eq. (29), requiring the coverage of prediction sets. However, it is not explicitly claimed but desired that a conformal prediction model can be adaptive for different conditions. For instance, we want the CP procedure can distinguish the difficulty of quantifying the prediction uncertainty of each input, and adaptively generate a larger prediction set as the difficulty increases [113]. In other words, the  $1 - \alpha$  coverage can be robust and stable no matter how the test domain changes. Let  $E_1, \dots, E_N$  denote the  $N$  sets of test inputs coming from the corresponding test domains, and we want the coverage guarantee to always hold that  $\forall e \in \{E_1, \dots, E_N\}$ :

$$\Pr(Y_{\text{test}} \in C(X_{\text{test}})) \geq 1 - \alpha, X_{\text{test}} \in e. \quad (40)$$

This test domain can be characterized by an explicit feature in input data or an underlying environment variable related to the data generation process. Fig. 2 shows the differences between marginal and conditional coverage with  $1 - \alpha = 0.8$ . The worst coverage among multiple domains is given by

$$\min_{e \in \{E_1, \dots, E_N\}} \frac{1}{|\mathcal{I}_e|} \sum_{i \in \mathcal{I}_e} \mathbb{1}\{Y_i \in C(X_i)\}, \quad (41)$$

where  $\mathcal{I}_e$  represent the sample index set of set  $e$  and  $|\mathcal{I}_e|$  denote the number of samples in set  $e$  [162], [163]. If the metric value is much lower than the expected coverage  $1 - \alpha$ , we say the CP procedure performs poorly on conditional coverage.

**Coverage Correctness.** The empirical coverage by split conformal prediction involves randomness due to the limited number of available samples and possibly biased data splitting. Running conformal prediction multiple times can help us

determine the correctness and stability of prediction coverage. With  $n$  labeled samples available, we can randomly split them into  $n_{\text{cal}}$  samples for calibration and  $n_{\text{val}}$  samples for validation, and calculate the coverage by

$$c_t = \frac{1}{n_{\text{val}}} \sum_{i=1}^{n_{\text{val}}} \mathbb{1}\{Y_{i,t} \in C(X_{i,t})\}, \quad (42)$$

where  $Y_{i,t}$  and  $X_{i,t}$  are the label and feature of the  $i$ -th element of  $n_{\text{val}}$  validation samples at  $t$ -th time splitting. After repeating for  $T$  times, the final averaged empirical coverage,  $\bar{c}$ , will be  $\frac{1}{T} \sum_{t=1}^T c_t$ . The variance of these empirical coverage values indicates the stability as  $\frac{1}{T} \sum_{t=1}^T (c_t - \bar{c})^2$ .

## VII. RESOURCES

This section compiles tutorials from prominent machine-learning conferences and open-source codes from some cited papers on related topics for convenient access.

## VIII. CONCLUSION AND FUTURE WORK

In this survey, we carefully reviewed the uncertainty quantification within graphical models, specifically focusing on Graph Neural Networks and Probabilistic Graphical Models. We examined existing methods for representing and handling uncertainty, including Bayesian representation learning, conformal prediction, calibration and so on. The domain of uncertainty in graphical models presents substantial opportunities for further innovation and advancement. Advancing our understanding of uncertainty modeling in graph-based systems will empower machine learning systems to make more reliable decisions in the presence of real-world noise. Such progress will not only improve the accuracy and safety of AI applications but also promote trust and encourage the broader adoption of these technologies in practical settings.

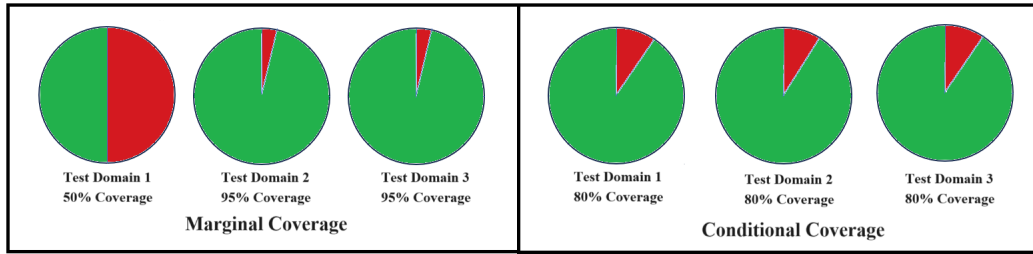


Fig. 2. Marginal Coverage vs Conditional Coverage with  $(1-\alpha)=0.8$ . Marginal coverage can only guarantee the coverage on the overall sample set, but conditional coverage can ensure at least  $1-\alpha$  coverage on different sub-domains

TABLE III  
OPEN-SOURCE CODES

Method	Model	Algorithm	Code Link
Bayesian Method	General Model	VAEs [46]	<a href="https://github.com/AntixK/PyTorch-VAE">https://github.com/AntixK/PyTorch-VAE</a>
		BNNs [47], [48]	<a href="https://github.com/Harry24k/bayesian-neural-network-pytorch">https://github.com/Harry24k/bayesian-neural-network-pytorch</a>
	Graphic Model	NETCONF [44]	<a href="https://dhivyaeswaran.github.io/code/netconf.zip">https://dhivyaeswaran.github.io/code/netconf.zip</a>
		GPN [45]	<a href="https://www.daml.in.tum.de/graph-postnet">https://www.daml.in.tum.de/graph-postnet</a>
		VGAE [50]	<a href="https://github.com/tkipf/gae">https://github.com/tkipf/gae</a>
		DGVAE [52]	<a href="https://github.com/xiyou3368/DGVAE">https://github.com/xiyou3368/DGVAE</a>
		SIG-VAE [51]	<a href="https://github.com/sigvae/SIGraphVAE">https://github.com/sigvae/SIGraphVAE</a>
		VGNAE [53]	<a href="https://github.com/SeongJinAhn/VGNAE">https://github.com/SeongJinAhn/VGNAE</a>
		Graphite [54]	<a href="https://github.com/ermongroup/graphite">https://github.com/ermongroup/graphite</a>
		VGRNN [57]	<a href="https://github.com/VGraphRNN/VGRNN">https://github.com/VGraphRNN/VGRNN</a>
		Bayesian GCNN [59]	<a href="https://github.com/huawei-noah/BGCN">https://github.com/huawei-noah/BGCN</a>
		Bayesian GCNN (node copying) [62]	<a href="https://github.com/floregol/BGCN_copying">https://github.com/floregol/BGCN_copying</a>
		S-BGCN-T-K [65]	<a href="https://github.com/zxj32/uncertainty-GNN">https://github.com/zxj32/uncertainty-GNN</a>
		VGCN [68]	<a href="https://github.com/ebonilla/VGCN">https://github.com/ebonilla/VGCN</a>
		GGP [77]	<a href="https://github.com/yincheng/GGP">https://github.com/yincheng/GGP</a>
		GPG [81]	<a href="https://www.kth.se/ise/research/reproduciblereasearch1.433797">https://www.kth.se/ise/research/reproduciblereasearch1.433797</a>
		DGPG [82]	<a href="https://github.com/naiqili/DGPG">https://github.com/naiqili/DGPG</a>
		FT-GP & WT-GP [83]	<a href="https://github.com/FelixOpolka/Graph-Classification-Gaussian-Processes-via-Spectral-Features">https://github.com/FelixOpolka/Graph-Classification-Gaussian-Processes-via-Spectral-Features</a>
		LNK [84]	<a href="https://github.com/wollschl/uncertainty_for_molecules">https://github.com/wollschl/uncertainty_for_molecules</a>
		GGPN [86]	<a href="https://github.com/sysu-gzchen/GGPN">https://github.com/sysu-gzchen/GGPN</a>
Conformal Prediction	General Model	CPCS [116]	<a href="https://github.com/ryantibs/conformal/tree/master/tibshirani2019">https://github.com/ryantibs/conformal/tree/master/tibshirani2019</a>
		CQR [114]	<a href="https://github.com/yromano/cqr">https://github.com/yromano/cqr</a>
		APS [112]	<a href="https://github.com/msesia/arc">https://github.com/msesia/arc</a>
		conformalbayes [164]	<a href="https://github.com/CoryMcCartan/conformalbayes">https://github.com/CoryMcCartan/conformalbayes</a>
		EnbPI [118]	<a href="https://github.com/hamrel-cxu/EnbPI">https://github.com/hamrel-cxu/EnbPI</a>
		CP with Missing Values [165]	<a href="https://github.com/mzaffran/ConformalPredictionMissingValues">https://github.com/mzaffran/ConformalPredictionMissingValues</a>
		LCP [115]	<a href="https://github.com/LeyingGuan/LCP">https://github.com/LeyingGuan/LCP</a>
		stabCP [166]	<a href="https://github.com/EugeneNdiaye/stable_conformal_prediction">https://github.com/EugeneNdiaye/stable_conformal_prediction</a>
		OQR [163]	<a href="https://github.com/Shai128/oqr">https://github.com/Shai128/oqr</a>
	Graphic Model	NAPS [125]	<a href="https://github.com/jase-clarkson/graph_cp">https://github.com/jase-clarkson/graph_cp</a>
		DAPS [123]	<a href="https://github.com/soroushzargar/DAPS">https://github.com/soroushzargar/DAPS</a>
		CF-GNN [167]	<a href="https://github.com/snap-stanford/conformalized-gnn">https://github.com/snap-stanford/conformalized-gnn</a>
		JuryGCN [124]	<a href="https://github.com/BlueWhaleZhou/JuryGCN_UQ">https://github.com/BlueWhaleZhou/JuryGCN_UQ</a>
Calibration	General Model	Dirichlet Calibration [159]	<a href="https://github.com/dirichletcal/dirichletcal.github.io">https://github.com/dirichletcal/dirichletcal.github.io</a>
		Calibrated Regression [128]	<a href="https://github.com/AnthonyRentsch/calibrated_regression">https://github.com/AnthonyRentsch/calibrated_regression</a>
		Focal Calibration [131]	<a href="https://github.com/torrvision/focal_calibration">https://github.com/torrvision/focal_calibration</a>
		Label Smoothing [132]	<a href="https://github.com/seominseok0429/label-smoothing-visualization-pytorch">https://github.com/seominseok0429/label-smoothing-visualization-pytorch</a>
		Spline Calibration [168]	<a href="https://github.com/kartikgupta-at-anu/spline-calibration">https://github.com/kartikgupta-at-anu/spline-calibration</a>
	Graphic Model	G- $\Delta$ UQ [152]	<a href="https://github.com/pujacomputes/gduq">https://github.com/pujacomputes/gduq</a>
		CaGCN [135]	<a href="https://github.com/BUPT-GAMMA/CaGCN">https://github.com/BUPT-GAMMA/CaGCN</a>
		GATS [136]	<a href="https://github.com/hans66hsu/GATS">https://github.com/hans66hsu/GATS</a>
		RBS [137]	<a href="https://github.com/liu-yushan/calGNN">https://github.com/liu-yushan/calGNN</a>
		HyperU-GCN [143]	<a href="https://github.com/xyang2316/HyperU-GCN">https://github.com/xyang2316/HyperU-GCN</a>

TABLE IV  
TUTORIALS ON UNCERTAINTY QUANTIFICATION AND GRAPHIC MODELS

Tutorial	$G$	Bayes	CP	Cal	OOD	Venues	Year
Graph Learning: Principles, Challenges, and Open Directions	✓					ICML	2024
Formalizing Robustness in Neural Networks: Explainability, Uncertainty, and Intervenability					✓	AAAI	2024
Distribution-Free Predictive Uncertainty Quantification: Strengths and Limits of Conformal Prediction			✓			ICML	2024
Graph Neural Networks: Foundation, Frontiers and Applications	✓					KDD	2023
Large-Scale Graph Neural Networks: The Past and New Frontiers	✓					KDD	2023
Hyperbolic Graph Neural Networks: A Tutorial on Methods and Applications	✓					KDD	2023
Fairness in Graph Machine Learning: Recent Advances and Future Prospectives	✓					KDD	2023
Graph Neural Networks: Foundation, Frontiers and Applications	✓					AAAI	2023
Temporal Graph Mining for Fraud Detection	✓					ICDM	2023
Recent Advances in Bayesian Optimization		✓				AAAI	2023
Uncertainty Quantification in Deep Learning		✓	✓	✓		KDD	2023
Modeling and Exploiting Data Heterogeneity under Distribution Shifts					✓	NeurIPS	2023
Trustworthy Graph Learning: Reliability, Explainability, and Privacy Protection	✓					KDD	2022
Algorithmic Fairness on Graphs: Methods and Trends	✓					KDD	2022
Automated Learning from Graph-Structured Data	✓					AAAI	2022
Fairness in Graph Mining: Metrics, Algorithms, and Applications	✓					ICDM	2022
Advances in Bayesian Optimization		✓				NeurIPS	2022
Bayesian Optimization: From Foundations to Advanced Topics		✓				AAAI	2022
Sampling as First-Order Optimization over a space of probability measures						ICML	2022
Graph Representation Learning: Foundations, Methods, Applications and Systems	✓					KDD	2021
Toward Explainable Deep Anomaly Detection					✓	KDD	2021
The Art of Gaussian Processes: Classical and Contemporary		✓				NeurIPS	2021
On Calibration and Out-of-Domain Generalization				✓	✓	ICLR	2021
Deep Graph Learning: Foundations, Advances and Applications	✓					KDD	2020
Differential Deep Learning on Graphs and its Applications	✓					AAAI	2020
Bayesian Deep Learning and a Probabilistic Perspective of Model Construction		✓				ICML	2020
Robust Deep Learning Methods for Anomaly Detection.					✓	KDD	2020
How to calibrate your neural network classifier: Getting true probabilities from a classification model				✓		KDD	2020
Practical Uncertainty Estimation and Out-of-Distribution Robustness in Deep Learning					✓	NeurIPS	2020
Graph Representation Learning	✓					AAAI	2019
Representation Learning on Graphs and Manifolds	✓					ICLR	2019
A Primer on PAC-Bayesian Learning		✓				ICML	2019
Deep Learning with Bayesian Principles		✓				NeurIPS	2019
Deep Bayesian Mining, Learning and Understanding		✓				KDD	2019
Deep Bayesian and Sequential Learning		✓				AAAI	2019
Variational Bayes and Beyond: Bayesian Inference for Big Data		✓				ICML	2018
Scalable Bayesian Inference		✓				NeurIPS	2018
Bayesian Incremental Learning for Deep Neural Networks		✓				ICLR	2018
Bayesian Approaches for Blackbox Optimization		✓				UAI	2018
Deep Probabilistic Modelling with Gaussian Processes		✓				NeurIPS	2017
Non-IID Learning					✓	KDD	2017
Bayesian Time Series Modeling: Structured Representations for Scalability		✓				ICML	2015
Optimal Algorithms for Learning Bayesian Network Structures		✓				UAI	2015
Computational Complexity of Bayesian Networks		✓				UAI	2015
Bayesian Posterior Inference in the Big Data Arena: An introduction to probabilistic programming		✓				ICML	2014
Approximate Bayesian Computation (ABC)		✓				NeurIPS	2013
Linear Programming Relaxations for Graphical Models	✓					NeurIPS	2011
Modern Bayesian Nonparametrics		✓				NeurIPS	2011

## REFERENCES

- [1] S. Rayana and L. Akoglu, "Collective opinion spam detection: Bridging review networks and metadata," in *Proceedings of the 21th acm sigkdd international conference on knowledge discovery and data mining*, 2015, pp. 985–994.
- [2] S. Noekhah, N. binti Salim, and N. H. Zakaria, "Opinion spam detection: Using multi-iterative graph-based model," *Information processing & management*, vol. 57, no. 1, p. 102140, 2020.
- [3] N. Agarwal, H. Liu, S. Murthy, A. Sen, and X. Wang, "A social identity approach to identify familiar strangers in a social network," in *Proceedings of the International AAAI Conference on Web and Social Media*, vol. 3, no. 1, 2009, pp. 2–9.
- [4] H. Zhang, G. Lu, M. Zhan, and B. Zhang, "Semi-supervised classification of graph convolutional networks with laplacian rank constraints," *Neural Processing Letters*, pp. 1–12, 2022.
- [5] T. N. Kipf and M. Welling, "Semi-supervised classification with graph convolutional networks," *arXiv preprint arXiv:1609.02907*, 2016.
- [6] W. Hamilton, Z. Ying, and J. Leskovec, "Inductive representation learning on large graphs," *NeurIPS*, 2017.
- [7] S. Wu, F. Sun, W. Zhang, X. Xie, and B. Cui, "Graph neural networks in recommender systems: a survey," *ACM Computing Surveys*, vol. 55, no. 5, pp. 1–37, 2022.
- [8] K. Gupta, A. Rahimi, T. Ajanthan, T. Mensink, C. Sminchescu, and R. Hartley, "Calibration of neural networks using splines," *arXiv preprint arXiv:2006.12800*, 2020.
- [9] C. Guo, G. Pleiss, Y. Sun, and K. Q. Weinberger, "On calibration of modern neural networks," in *International conference on machine learning*. PMLR, 2017, pp. 1321–1330.
- [10] S. Huang, Y. Wang, L. Mou, H. Zhang, H. Zhu, C. Yu, and B. Zheng, "Mbct: Tree-based feature-aware binning for individual uncertainty calibration," in *Proceedings of the ACM Web Conference 2022*, 2022, pp. 2236–2246.
- [11] A. Strokach, D. Becerra, C. Corbi-Verge, A. Perez-Riba, and P. M. Kim, "Fast and flexible protein design using deep graph neural networks," *Cell systems*, vol. 11, no. 4, pp. 402–411, 2020.
- [12] M. Réau, N. Renaud, L. C. Xue, and A. M. Bonvin, "DeepRank-gnn: a graph neural network framework to learn patterns in protein–protein interfaces," *Bioinformatics*, vol. 39, no. 1, p. btac759, 2023.
- [13] K. Jha, S. Saha, and H. Singh, "Prediction of protein–protein interaction using graph neural networks," *Scientific Reports*, vol. 12, no. 1, p. 8360, 2022.
- [14] F. Wang, Y. Liu, K. Liu, Y. Wang, S. Medya, and P. S. Yu, "Uncertainty in graph neural networks: A survey," *arXiv preprint arXiv:2403.07185*, 2024.
- [15] S. Seoni, V. Jahmunah, M. Salvi, P. D. Barua, F. Molinari, and U. R. Acharya, "Application of uncertainty quantification to artificial intelligence in healthcare: A review of last decade (2013–2023)," *Computers in Biology and Medicine*, p. 107441, 2023.
- [16] X. Tang, G. Zhong, S. Li, K. Yang, K. Shu, D. Cao, and X. Lin, "Uncertainty-aware decision-making for autonomous driving at uncontrolled intersections," *IEEE Transactions on Intelligent Transportation Systems*, 2023.
- [17] M. Abdar, F. Pourpanah, S. Hussain, D. Rezazadegan, L. Liu, M. Ghavamzadeh, P. Fieguth, X. Cao, A. Khosravi, U. R. Acharya et al., "A review of uncertainty quantification in deep learning: Techniques, applications and challenges," *Information fusion*, vol. 76, pp. 243–297, 2021.
- [18] J. Gawlikowski, C. R. N. Tassi, M. Ali, J. Lee, M. Humt, J. Feng, A. Kruspe, R. Triebel, P. Jung, R. Roscher et al., "A survey of uncertainty in deep neural networks," *Artificial Intelligence Review*, vol. 56, no. Suppl 1, pp. 1513–1589, 2023.
- [19] J. Mena, O. Pujol, and J. Vitrià, "A survey on uncertainty estimation in deep learning classification systems from a bayesian perspective," *ACM Computing Surveys (CSUR)*, vol. 54, no. 9, pp. 1–35, 2021.
- [20] H. Wang and D.-Y. Yeung, "A survey on bayesian deep learning," *ACM computing surveys (csur)*, vol. 53, no. 5, pp. 1–37, 2020.
- [21] A. F. Psaros, X. Meng, Z. Zou, L. Guo, and G. E. Karniadakis, "Uncertainty quantification in scientific machine learning: Methods, metrics, and comparisons," *Journal of Computational Physics*, vol. 477, p. 111902, 2023.
- [22] C. Gruber, P. O. Schenk, M. Schierholz, F. Kreuter, and G. Kauermann, "Sources of uncertainty in machine learning—a statisticians' view," *arXiv preprint arXiv:2305.16703*, 2023.
- [23] E. Hüllermeier and W. Waegeman, "Aleatoric and epistemic uncertainty in machine learning: An introduction to concepts and methods," *Machine learning*, vol. 110, no. 3, pp. 457–506, 2021.
- [24] C. Ning and F. You, "Optimization under uncertainty in the era of big data and deep learning: When machine learning meets mathematical programming," *Computers & Chemical Engineering*, vol. 125, pp. 434–448, 2019.
- [25] S. Gupta and A. Gupta, "Dealing with noise problem in machine learning data-sets: A systematic review," *Procedia Computer Science*, vol. 161, pp. 466–474, 2019.
- [26] C. M. Bishop and N. M. Nasrabadi, *Pattern recognition and machine learning*. Springer, 2006, vol. 4, no. 4.
- [27] M. I. Jordan, "Graphical models," 2004.
- [28] K. Xu, W. Hu, J. Leskovec, and S. Jegelka, "How powerful are graph neural networks?" *ICLR*, 2019.
- [29] A. Der Kiureghian and O. Ditlevsen, "Aleatory or epistemic? does it matter?" *Structural safety*, vol. 31, no. 2, pp. 105–112, 2009.
- [30] I. Hacking, *The emergence of probability: A philosophical study of early ideas about probability, induction and statistical inference*. Cambridge University Press, 2006.
- [31] A. Kendall and Y. Gal, "What uncertainties do we need in bayesian deep learning for computer vision?" *Advances in neural information processing systems*, vol. 30, 2017.
- [32] M. Valdenegro-Toro and D. Saromo, "A deeper look into aleatoric and epistemic uncertainty disentanglement," 2022.
- [33] S. Munikoti, D. Agarwal, L. Das, and B. Natarajan, "A general framework for quantifying aleatoric and epistemic uncertainty in graph neural networks," *Neurocomputing*, vol. 521, pp. 1–10, 2023.
- [34] S. C. Hora, "Aleatory and epistemic uncertainty in probability elicitation with an example from hazardous waste management," *Reliability Engineering & System Safety*, vol. 54, no. 2-3, pp. 217–223, 1996.
- [35] V. Chernozhukov, C. Cinelli, W. K. Newey, A. Sharma, and V. Syrgkanis, "Omitted variable bias in machine learned causal models," cemmap working paper, Tech. Rep., 2021.
- [36] J. R. Busenbark, H. Yoon, D. L. Gamache, and M. C. Withers, "Omitted variable bias: Examining management research with the impact threshold of a confounding variable (itcv)," *Journal of Management*, vol. 48, no. 1, pp. 17–48, 2022.
- [37] C. Cinelli and C. Hazlett, "Making sense of sensitivity: Extending omitted variable bias," *Journal of the Royal Statistical Society Series B: Statistical Methodology*, vol. 82, no. 1, pp. 39–67, 2020.
- [38] C. G. Northcutt, A. Athalye, and J. Mueller, "Pervasive label errors in test sets destabilize machine learning benchmarks," *arXiv preprint arXiv:2103.14749*, 2021.
- [39] R. J. Little and D. B. Rubin, *Statistical analysis with missing data*. John Wiley & Sons, 2019, vol. 793.
- [40] S. Lahlou, M. Jain, H. Nekoei, V. I. Butoi, P. Bertin, J. Rector-Brooks, M. Korablyov, and Y. Bengio, "Deup: Direct epistemic uncertainty prediction," *arXiv preprint arXiv:2102.08501*, 2021.
- [41] V.-L. Nguyen, S. Destercke, and E. Hüllermeier, "Epistemic uncertainty sampling," in *Advances in Knowledge Discovery and Data Mining: 19th Pacific-Asia Conference, PAKDD 2015, Ho Chi Minh City, Vietnam, May 19-22, 2015, Proceedings, Part 1*. Springer, 2019, pp. 72–86.
- [42] Z. Huang, H. Lam, and H. Zhang, "Quantifying epistemic uncertainty in deep learning," *arXiv preprint arXiv:2110.12122*, 2021.
- [43] Y. Yamaguchi, C. Faloutsos, and H. Kitagawa, "Socnl: Bayesian label propagation with confidence," in *Advances in Knowledge Discovery and Data Mining: 19th Pacific-Asia Conference, PAKDD 2015, Ho Chi Minh City, Vietnam, May 19-22, 2015, Proceedings, Part 1*. Springer, 2015, pp. 633–645.
- [44] D. Eswaran, S. Günnemann, and C. Faloutsos, "The power of certainty: A dirichlet-multinomial model for belief propagation," in *Proceedings of the 2017 SIAM International Conference on Data Mining*. SIAM, 2017, pp. 144–152.
- [45] M. Stadler, B. Charpentier, S. Geisler, D. Zügner, and S. Günnemann, "Graph posterior network: Bayesian predictive uncertainty for node classification," *Advances in Neural Information Processing Systems*, vol. 34, pp. 18033–18048, 2021.
- [46] D. P. Kingma and M. Welling, "Auto-encoding variational bayes," *arXiv preprint arXiv:1312.6114*, 2013.
- [47] J. Lampinen and A. Vehtari, "Bayesian approach for neural networks—review and case studies," *Neural networks*, vol. 14, no. 3, pp. 257–274, 2001.
- [48] D. M. Titterton, "Bayesian methods for neural networks and related models," *Statistical science*, pp. 128–139, 2004.
- [49] Y. Gal and Z. Ghahramani, "Dropout as a bayesian approximation: Representing model uncertainty in deep learning," in *international conference on machine learning*. PMLR, 2016, pp. 1050–1059.
- [50] T. N. Kipf and M. Welling, "Variational graph auto-encoders," *arXiv preprint arXiv:1611.07308*, 2016.

- [51] A. Hasanzadeh, E. Hajiramezanali, K. Narayanan, N. Duffield, M. Zhou, and X. Qian, "Semi-implicit graph variational auto-encoders," *Advances in neural information processing systems*, vol. 32, 2019.
- [52] J. Li, J. Yu, J. Li, H. Zhang, K. Zhao, Y. Rong, H. Cheng, and J. Huang, "Dirichlet graph variational autoencoder," *Advances in Neural Information Processing Systems*, vol. 33, pp. 5274–5283, 2020.
- [53] S. J. Ahn and M. Kim, "Variational graph normalized autoencoders," in *Proceedings of the 30th ACM international conference on information & knowledge management*, 2021, pp. 2827–2831.
- [54] A. Grover, A. Zweig, and S. Ermon, "Graphite: Iterative generative modeling of graphs," in *International conference on machine learning*. PMLR, 2019, pp. 2434–2444.
- [55] M. Simonovsky and N. Komodakis, "Graphvae: Towards generation of small graphs using variational autoencoders," in *Artificial Neural Networks and Machine Learning–ICANN 2018: 27th International Conference on Artificial Neural Networks, Rhodes, Greece, October 4–7, 2018, Proceedings, Part I 27*. Springer, 2018, pp. 412–422.
- [56] W. L. Hamilton, *Graph representation learning*. Morgan & Claypool Publishers, 2020.
- [57] E. Hajiramezanali, A. Hasanzadeh, K. Narayanan, N. Duffield, M. Zhou, and X. Qian, "Variational graph recurrent neural networks," *Advances in neural information processing systems*, vol. 32, 2019.
- [58] L. Sun, Z. Zhang, J. Zhang, F. Wang, H. Peng, S. Su, and P. S. Yu, "Hyperbolic variational graph neural network for modeling dynamic graphs," in *Proceedings of the AAAI Conference on Artificial Intelligence*, vol. 35, no. 5, 2021, pp. 4375–4383.
- [59] Y. Zhang, S. Pal, M. Coates, and D. Ustebay, "Bayesian graph convolutional neural networks for semi-supervised classification," in *Proceedings of the AAAI conference on artificial intelligence*, vol. 33, no. 01, 2019, pp. 5829–5836.
- [60] W. Li, S. Ahn, and M. Welling, "Scalable mcmc for mixed membership stochastic blockmodels," in *Artificial Intelligence and Statistics*. PMLR, 2016, pp. 723–731.
- [61] P. K. Gopalan, S. Gerrish, M. Freedman, D. Blei, and D. Mimno, "Scalable inference of overlapping communities," *Advances in Neural Information Processing Systems*, vol. 25, 2012.
- [62] S. Pal, F. Regol, and M. Coates, "Bayesian graph convolutional neural networks using node copying," in *Proceedings of the 36th International Conference on Machine Learning, Workshop on Learning and Reasoning with Graph-Structured Representations*. ICML, 2019.
- [63] S. Pal, S. Malekmohammadi, F. Regol, Y. Zhang, Y. Xu, and M. Coates, "Non parametric graph learning for bayesian graph neural networks," in *Conference on uncertainty in artificial intelligence*. PMLR, 2020, pp. 1318–1327.
- [64] Z. Xu, C. Lawrence, A. Shaker, and R. Siarheyev, "Uncertainty propagation in node classification," in *2022 IEEE International Conference on Data Mining (ICDM)*. IEEE, 2022, pp. 1275–1280.
- [65] X. Zhao, F. Chen, S. Hu, and J.-H. Cho, "Uncertainty aware semi-supervised learning on graph data," *Advances in Neural Information Processing Systems*, vol. 33, pp. 12 827–12 836, 2020.
- [66] S. Depeweg, J.-M. Hernandez-Lobato, F. Doshi-Velez, and S. Udluft, "Decomposition of uncertainty in bayesian deep learning for efficient and risk-sensitive learning," in *International Conference on Machine Learning*. PMLR, 2018, pp. 1184–1193.
- [67] A. Malinin and M. Gales, "Predictive uncertainty estimation via prior networks," *Advances in neural information processing systems*, vol. 31, 2018.
- [68] P. Elinas, E. V. Bonilla, and L. Tiao, "Variational inference for graph convolutional networks in the absence of graph data and adversarial settings," *Advances in Neural Information Processing Systems*, vol. 33, pp. 18 648–18 660, 2020.
- [69] E. Jang, S. Gu, and B. Poole, "Categorical reparameterization with gumbel-softmax," *arXiv preprint arXiv:1611.01144*, 2016.
- [70] C. J. Maddison, A. Mnih, and Y. W. Teh, "The concrete distribution: A continuous relaxation of discrete random variables," *arXiv preprint arXiv:1611.00712*, 2016.
- [71] C. K. Williams and C. E. Rasmussen, *Gaussian processes for machine learning*. MIT press Cambridge, MA, 2006, vol. 2, no. 3.
- [72] J. Quinero-Candela and C. E. Rasmussen, "A unifying view of sparse approximate gaussian process regression," *The Journal of Machine Learning Research*, vol. 6, pp. 1939–1959, 2005.
- [73] M. Titsias, "Variational learning of inducing variables in sparse gaussian processes," in *Artificial intelligence and statistics*. PMLR, 2009, pp. 567–574.
- [74] A. Rahimi and B. Recht, "Random features for large-scale kernel machines," *Advances in neural information processing systems*, vol. 20, 2007.
- [75] A. Damianou and N. D. Lawrence, "Deep gaussian processes," in *Artificial intelligence and statistics*. PMLR, 2013, pp. 207–215.
- [76] J. Bradshaw, A. G. d. G. Matthews, and Z. Ghahramani, "Adversarial examples, uncertainty, and transfer testing robustness in gaussian process hybrid deep networks," *arXiv preprint arXiv:1707.02476*, 2017.
- [77] Y. C. Ng, N. Colombo, and R. Silva, "Bayesian semi-supervised learning with graph gaussian processes," *Advances in Neural Information Processing Systems*, vol. 31, 2018.
- [78] Z.-Y. Liu, S.-Y. Li, S. Chen, Y. Hu, and S.-J. Huang, "Uncertainty aware graph gaussian process for semi-supervised learning," in *Proceedings of the AAAI Conference on Artificial Intelligence*, vol. 34, no. 04, 2020, pp. 4957–4964.
- [79] J. Hu, J. Shen, B. Yang, and L. Shao, "Infinitely wide graph convolutional networks: semi-supervised learning via gaussian processes," *arXiv preprint arXiv:2002.12168*, 2020.
- [80] F. Opolka, Y.-C. Zhi, P. Lio, and X. Dong, "Adaptive gaussian processes on graphs via spectral graph wavelets," in *International Conference on Artificial Intelligence and Statistics*. PMLR, 2022, pp. 4818–4834.
- [81] A. Venkitaraman, S. Chatterjee, and P. Handel, "Gaussian processes over graphs," in *ICASSP 2020-2020 IEEE International Conference on Acoustics, Speech and Signal Processing (ICASSP)*. IEEE, 2020, pp. 5640–5644.
- [82] N. Li, W. Li, J. Sun, Y. Gao, Y. Jiang, and S.-T. Xia, "Stochastic deep gaussian processes over graphs," *Advances in Neural Information Processing Systems*, vol. 33, pp. 5875–5886, 2020.
- [83] F. L. Opolka, Y.-C. Zhi, P. Liò, and X. Dong, "Graph classification gaussian processes via spectral features," in *Uncertainty in Artificial Intelligence*. PMLR, 2023, pp. 1575–1585.
- [84] T. Wollschläger, N. Gao, B. Charpentier, M. A. Ketata, and S. Günnemann, "Uncertainty estimation for molecules: Desiderata and methods," in *International Conference on Machine Learning*. PMLR, 2023, pp. 37 133–37 156.
- [85] F. L. Opolka and P. Liò, "Graph convolutional gaussian processes for link prediction," *arXiv preprint arXiv:2002.04337*, 2020.
- [86] G. Chen, J. Fang, Z. Meng, Q. Zhang, and S. Liang, "Multi-relational graph representation learning with bayesian gaussian process network," in *Proceedings of the AAAI Conference on Artificial Intelligence*, vol. 36, no. 5, 2022, pp. 5530–5538.
- [87] M. Girolami and S. Rogers, "Variational bayesian multinomial probit regression with gaussian process priors," *Neural Computation*, vol. 18, no. 8, pp. 1790–1817, 2006.
- [88] M. Van der Wilk, C. E. Rasmussen, and J. Hensman, "Convolutional gaussian processes," *Advances in neural information processing systems*, vol. 30, 2017.
- [89] H. Li, X. Wang, Z. Zhang, and W. Zhu, "Out-of-distribution generalization on graphs: A survey," *arXiv preprint arXiv:2202.07987*, 2022.
- [90] J. C. Duchi and H. Namkoong, "Learning models with uniform performance via distributionally robust optimization," *The Annals of Statistics*, vol. 49, no. 3, pp. 1378–1406, 2021.
- [91] G. Bayraksan and D. K. Love, "Data-driven stochastic programming using phi-divergences," in *The operations research revolution*. Informa, 2015, pp. 1–19.
- [92] A. Ben-Tal, D. Den Hertog, A. De Waegenaere, B. Melenberg, and G. Rennen, "Robust solutions of optimization problems affected by uncertain probabilities," *Management Science*, vol. 59, no. 2, pp. 341–357, 2013.
- [93] L. Pardo, *Statistical inference based on divergence measures*. Chapman and Hall/CRC, 2018.
- [94] Z. Hu and L. J. Hong, "Kullback-leibler divergence constrained distributionally robust optimization," *Available at Optimization Online*, vol. 1, no. 2, p. 9, 2013.
- [95] J. Wu, J. Chen, J. Wu, W. Shi, X. Wang, and X. He, "Understanding contrastive learning via distributionally robust optimization," *Advances in Neural Information Processing Systems*, vol. 36, 2024.
- [96] R. Gao and A. Kleywegt, "Distributionally robust stochastic optimization with wasserstein distance," *Mathematics of Operations Research*, vol. 48, no. 2, pp. 603–655, 2023.
- [97] P. Mohajerin Esfahani and D. Kuhn, "Data-driven distributionally robust optimization using the wasserstein metric: Performance guarantees and tractable reformulations," *Mathematical Programming*, vol. 171, no. 1, pp. 115–166, 2018.
- [98] C. Zhao and Y. Guan, "Data-driven risk-averse stochastic optimization with wasserstein metric," *Operations Research Letters*, vol. 46, no. 2, pp. 262–267, 2018.
- [99] A. Sadeghi, M. Ma, B. Li, and G. B. Giannakis, "Distributionally robust semi-supervised learning over graphs," *arXiv preprint arXiv:2110.10582*, 2021.



- [100] X. Zhang, Y. Xu, Q. Liu, Z. Liu, J. Lu, and Q. Wang, “Robust graph learning under wasserstein uncertainty,” *arXiv preprint arXiv:2105.04210*, 2021.
- [101] S. Chen, K. Ding, and S. Zhu, “Uncertainty-aware robust learning on noisy graphs,” *arXiv preprint arXiv:2306.08210*, 2023.
- [102] M. Staib and S. Jegelka, “Distributionally robust optimization and generalization in kernel methods,” *Advances in Neural Information Processing Systems*, vol. 32, 2019.
- [103] E. Erdoğan and G. Iyengar, “Ambiguous chance constrained problems and robust optimization,” *Mathematical Programming*, vol. 107, pp. 37–61, 2006.
- [104] F. Feng, X. He, J. Tang, and T.-S. Chua, “Graph adversarial training: Dynamically regularizing based on graph structure,” *IEEE Transactions on Knowledge and Data Engineering*, vol. 33, no. 6, pp. 2493–2504, 2019.
- [105] Y. Wu, A. Bojchevski, and H. Huang, “Adversarial weight perturbation improves generalization in graph neural networks,” in *Proceedings of the AAAI Conference on Artificial Intelligence*, vol. 37, no. 9, 2023, pp. 10417–10425.
- [106] H. Xue, K. Zhou, T. Chen, K. Guo, X. Hu, Y. Chang, and X. Wang, “Cap: Co-adversarial perturbation on weights and features for improving generalization of graph neural networks,” *arXiv preprint arXiv:2110.14855*, 2021.
- [107] W. Hu, B. Liu, J. Gomes, M. Zitnik, P. Liang, V. Pande, and J. Leskovec, “Strategies for pre-training graph neural networks,” *arXiv preprint arXiv:1905.12265*, 2019.
- [108] Y. You, T. Chen, Y. Sui, T. Chen, Z. Wang, and Y. Shen, “Graph contrastive learning with augmentations,” *Advances in neural information processing systems*, vol. 33, pp. 5812–5823, 2020.
- [109] J. Qiu, Q. Chen, Y. Dong, J. Zhang, H. Yang, M. Ding, K. Wang, and J. Tang, “Gcc: Graph contrastive coding for graph neural network pre-training,” in *Proceedings of the 26th ACM SIGKDD international conference on knowledge discovery & data mining*, 2020, pp. 1150–1160.
- [110] Y. Zhu, Y. Xu, F. Yu, Q. Liu, S. Wu, and L. Wang, “Deep graph contrastive representation learning,” *arXiv preprint arXiv:2006.04131*, 2020.
- [111] V. Vovk, A. Gammerman, and G. Shafer, *Algorithmic learning in a random world*. Springer, 2005, vol. 29.
- [112] Y. Romano, M. Sesia, and E. Candes, “Classification with valid and adaptive coverage,” *Advances in Neural Information Processing Systems*, vol. 33, pp. 3581–3591, 2020.
- [113] A. Angelopoulos, S. Bates, J. Malik, and M. I. Jordan, “Uncertainty sets for image classifiers using conformal prediction,” *arXiv preprint arXiv:2009.14193*, 2020.
- [114] Y. Romano, E. Patterson, and E. Candes, “Conformalized quantile regression,” *Advances in neural information processing systems*, vol. 32, 2019.
- [115] L. Guan, “Localized conformal prediction: A generalized inference framework for conformal prediction,” *Biometrika*, vol. 110, no. 1, pp. 33–50, 2023.
- [116] R. J. Tibshirani, R. Foygel Barber, E. Candes, and A. Ramdas, “Conformal prediction under covariate shift,” *Advances in neural information processing systems*, vol. 32, 2019.
- [117] I. Gibbs and E. J. Candès, “Adaptive conformal inference under distribution shift,” in *Neural Information Processing Systems*, 2021. [Online]. Available: <https://api.semanticscholar.org/CorpusID:235266057>
- [118] C. Xu and Y. Xie, “Conformal prediction interval for dynamic time-series,” in *International Conference on Machine Learning*. PMLR, 2021, pp. 11559–11569.
- [119] M. Cauchois, S. Gupta, A. Ali, and J. C. Duchi, “Robust validation: Confident predictions even when distributions shift,” *Journal of the American Statistical Association*, pp. 1–66, 2024.
- [120] A. Gendler, T.-W. Weng, L. Daniel, and Y. Romano, “Adversarially robust conformal prediction,” in *International Conference on Learning Representations*, 2021.
- [121] X. Zou and W. Liu, “Coverage-guaranteed prediction sets for out-of-distribution data,” in *Proceedings of the AAAI Conference on Artificial Intelligence*, vol. 38, no. 15, 2024, pp. 17263–17270.
- [122] R. F. Barber, E. J. Candès, A. Ramdas, and R. J. Tibshirani, “Conformal prediction beyond exchangeability,” *The Annals of Statistics*, vol. 51, no. 2, pp. 816–845, 2023.
- [123] S. H. Zargarbashi, S. Antonelli, and A. Bojchevski, “Conformal prediction sets for graph neural networks,” in *International Conference on Machine Learning*. PMLR, 2023, pp. 12292–12318.
- [124] J. Kang, Q. Zhou, and H. Tong, “Jurycn: quantifying jackknife uncertainty on graph convolutional networks,” in *Proceedings of the 28th ACM SIGKDD Conference on Knowledge Discovery and Data Mining*, 2022, pp. 742–752.
- [125] J. Clarkson, “Distribution free prediction sets for node classification,” in *International Conference on Machine Learning*. PMLR, 2023, pp. 6268–6278.
- [126] B. Zadrozny and C. Elkan, “Obtaining calibrated probability estimates from decision trees and naive bayesian classifiers,” in *ICML*, vol. 1, 2001, pp. 609–616.
- [127] —, “Transforming classifier scores into accurate multiclass probability estimates,” in *Proceedings of the eighth ACM SIGKDD international conference on Knowledge discovery and data mining*, 2002, pp. 694–699.
- [128] V. Kuleshov, N. Fenner, and S. Ermon, “Accurate uncertainties for deep learning using calibrated regression,” in *International conference on machine learning*. PMLR, 2018, pp. 2796–2804.
- [129] J. Platt *et al.*, “Probabilistic outputs for support vector machines and comparisons to regularized likelihood methods,” *Advances in large margin classifiers*, vol. 10, no. 3, pp. 61–74, 1999.
- [130] R. Krishnan and O. Tickoo, “Improving model calibration with accuracy versus uncertainty optimization,” *Advances in Neural Information Processing Systems*, vol. 33, pp. 18237–18248, 2020.
- [131] J. Mukhoti, V. Kulharia, A. Sanyal, S. Golodetz, P. Torr, and P. Dokania, “Calibrating deep neural networks using focal loss,” *Advances in Neural Information Processing Systems*, vol. 33, pp. 15288–15299, 2020.
- [132] R. Müller, S. Kornblith, and G. E. Hinton, “When does label smoothing help?” *Advances in neural information processing systems*, vol. 32, 2019.
- [133] T.-Y. Lin, P. Goyal, R. Girshick, K. He, and P. Dollár, “Focal loss for dense object detection,” in *Proceedings of the IEEE international conference on computer vision*, 2017, pp. 2980–2988.
- [134] L. Teixeira, B. Jalaian, and B. Ribeiro, “Are graph neural networks miscalibrated?” *arXiv preprint arXiv:1905.02296*, 2019.
- [135] X. Wang, H. Liu, C. Shi, and C. Yang, “Be confident! towards trustworthy graph neural networks via confidence calibration,” *Advances in Neural Information Processing Systems*, vol. 34, pp. 23768–23779, 2021.
- [136] H. H.-H. Hsu, Y. Shen, C. Tomani, and D. Cremers, “What makes graph neural networks miscalibrated?” *Advances in Neural Information Processing Systems*, vol. 35, pp. 13775–13786, 2022.
- [137] T. Liu, Y. Liu, M. Hildebrandt, M. Joblin, H. Li, and V. Tresp, “On calibration of graph neural networks for node classification,” in *2022 International Joint Conference on Neural Networks (IJCNN)*. IEEE, 2022, pp. 1–8.
- [138] M. Wang, H. Yang, and Q. Cheng, “Gcl: Graph calibration loss for trustworthy graph neural network,” in *Proceedings of the 30th ACM International Conference on Multimedia*, 2022, pp. 988–996.
- [139] F. Kupperts, J. Kronenberger, A. Shantia, and A. Haselhoff, “Multivariate confidence calibration for object detection,” in *Proceedings of the IEEE/CVF conference on computer vision and pattern recognition workshops*, 2020, pp. 326–327.
- [140] I. Vos, I. Bhat, B. Velthuis, Y. Ruigrok, and H. Kuijff, “Calibration techniques for node classification using graph neural networks on medical image data,” in *Medical Imaging with Deep Learning*. PMLR, 2024, pp. 1211–1224.
- [141] P. Mody, N. F. Chaves-de Plaza, K. Hildebrandt, and M. Staring, “Improving error detection in deep learning based radiotherapy autoutlining using bayesian uncertainty,” in *International Workshop on Uncertainty for Safe Utilization of Machine Learning in Medical Imaging*. Springer, 2022, pp. 70–79.
- [142] S. Fort, H. Hu, and B. Lakshminarayanan, “Deep ensembles: A loss landscape perspective,” *arXiv preprint arXiv:1912.02757*, 2019.
- [143] X. Yang, J. Wang, X. Zhao, S. Li, and Z. Tao, “Calibrate automated graph neural network via hyperparameter uncertainty,” in *Proceedings of the 31st ACM International Conference on Information & Knowledge Management*, 2022, pp. 4640–4644.
- [144] E. Dai and S. Wang, “Say no to the discrimination: Learning fair graph neural networks with limited sensitive attribute information,” in *Proceedings of the 14th ACM International Conference on Web Search and Data Mining*, 2021, pp. 680–688.
- [145] D. Zhu, Z. Zhang, P. Cui, and W. Zhu, “Robust graph convolutional networks against adversarial attacks,” in *Proceedings of the 25th ACM SIGKDD international conference on knowledge discovery & data mining*, 2019, pp. 1399–1407.

- [146] C. Agarwal, H. Lakkaraju, and M. Zitnik, "Towards a unified framework for fair and stable graph representation learning," in *Uncertainty in Artificial Intelligence*. PMLR, 2021, pp. 2114–2124.
- [147] X. Zhang, L. Zhang, B. Jin, and X. Lu, "A multi-view confidence-calibrated framework for fair and stable graph representation learning," in *2021 IEEE International Conference on Data Mining (ICDM)*. IEEE, 2021, pp. 1493–1498.
- [148] M. Zhang and Y. Chen, "Link prediction based on graph neural networks," *Advances in neural information processing systems*, vol. 31, 2018.
- [149] E. Nascimento, D. Mesquita, S. Kaskio, and A. H. Souza, "In-n-out: Calibrating graph neural networks for link prediction," *arXiv preprint arXiv:2403.04605*, 2024.
- [150] J. Thiagarajan, R. Anirudh, V. S. Narayanaswamy, and T. Bremer, "Single model uncertainty estimation via stochastic data centering," *Advances in Neural Information Processing Systems*, vol. 35, pp. 8662–8674, 2022.
- [151] P. Trivedi, D. Koutra, and J. J. Thiagarajan, "On estimating link prediction uncertainty using stochastic centering," in *ICASSP 2024 - 2024 IEEE International Conference on Acoustics, Speech and Signal Processing (ICASSP)*, 2024, pp. 6810–6814.
- [152] P. Trivedi, M. Heimann, R. Anirudh, D. Koutra, and J. J. Thiagarajan, "Accurate and scalable estimation of epistemic uncertainty for graph neural networks," in *The Twelfth International Conference on Learning Representations*, 2024. [Online]. Available: <https://openreview.net/forum?id=ZL6yd6N1S2>
- [153] V. P. Dwivedi, C. K. Joshi, A. T. Luu, T. Laurent, Y. Bengio, and X. Bresson, "Benchmarking graph neural networks," *Journal of Machine Learning Research*, vol. 24, no. 43, pp. 1–48, 2023.
- [154] B. Knyazev, G. W. Taylor, and M. Amer, "Understanding attention and generalization in graph neural networks," *Advances in neural information processing systems*, vol. 32, 2019.
- [155] P. Veličković, G. Cucurull, A. Casanova, A. Romero, P. Lio, and Y. Bengio, "Graph attention networks," *arXiv preprint arXiv:1710.10903*, 2017.
- [156] R. Achanta, A. Shaji, K. Smith, A. Lucchi, P. Fua, and S. Süsstrunk, "Slic superpixels compared to state-of-the-art superpixel methods," *IEEE transactions on pattern analysis and machine intelligence*, vol. 34, no. 11, pp. 2274–2282, 2012.
- [157] A. Niculescu-Mizil and R. Caruana, "Predicting good probabilities with supervised learning," in *Proceedings of the 22nd international conference on Machine learning*, 2005, pp. 625–632.
- [158] M. P. Naeni, G. Cooper, and M. Hauskrecht, "Obtaining well calibrated probabilities using bayesian binning," in *Proceedings of the AAAI conference on artificial intelligence*, vol. 29, no. 1, 2015.
- [159] M. Kull, M. Perello Nieto, M. Kängsepp, T. Silva Filho, H. Song, and P. Flach, "Beyond temperature scaling: Obtaining well-calibrated multi-class probabilities with dirichlet calibration," *Advances in neural information processing systems*, vol. 32, 2019.
- [160] H. H.-H. Hsu, Y. Shen, and D. Cremers, "A graph is more than its nodes: Towards structured uncertainty-aware learning on graphs," *arXiv preprint arXiv:2210.15575*, 2022.
- [161] G. W. Brier, "Verification of forecasts expressed in terms of probability," *Monthly weather review*, vol. 78, no. 1, pp. 1–3, 1950.
- [162] M. Cauchois, S. Gupta, and J. C. Duchi, "Knowing what you know: valid and validated confidence sets in multiclass and multilabel prediction," *Journal of machine learning research*, vol. 22, no. 81, pp. 1–42, 2021.
- [163] S. Feldman, S. Bates, and Y. Romano, "Improving conditional coverage via orthogonal quantile regression," *Advances in neural information processing systems*, vol. 34, pp. 2060–2071, 2021.
- [164] R. F. Barber, E. J. Candès, A. Ramdas, and R. J. Tibshirani, "Predictive inference with the jackknife+," *The Annals of Statistics*, 2019. [Online]. Available: <https://api.semanticscholar.org/CorpusID:147704029>
- [165] M. Zaffran, A. Dieuleveut, J. Josse, and Y. Romano, "Conformal prediction with missing values," in *International Conference on Machine Learning*. PMLR, 2023, pp. 40 578–40 604.
- [166] E. Ndiaye, "Stable conformal prediction sets," in *International Conference on Machine Learning*. PMLR, 2022, pp. 16 462–16 479.
- [167] K. Huang, Y. Jin, E. Candès, and J. Leskovec, "Uncertainty quantification over graph with conformalized graph neural networks," *arXiv preprint arXiv:2305.14535*, 2023.
- [168] K. Gupta, A. Rahimi, T. Ajanthan, T. Mensink, C. Sminchisescu, and R. Hartley, "Calibration of neural networks using splines," in *International Conference on Learning Representations*, 2021. [Online]. Available: <https://openreview.net/forum?id=eQe8DEWNN2W>